Pion-Nucleus Scattering in the (3,3) Resonance Region*

Carl B. Dover
Physics Department, Brookhaven National Laboratory, Upton, New York 11973

and

R. H. Lemmer
Physics Department, Rand Afrikaans University, Johannesburg, South Africa

(Received 7 December 1972)

A many-body formulation of pion-nucleus scattering in the (3,3) resonance region is presented. It is shown that the self-energy (optical potential) of a pion propagating through a Fermi gas of nucleons can be expressed as an integral over density of an effective pion-nucleon forward-scattering amplitude $f(kq;kq)$ *in the medium*. Using a pseudoscalar pion-nucleon interaction, one finds that $f(kq;kq)$ satisfies a modified form of the standard Chew-Low equation for pion-nucleon scattering. The effect of the medium is twofold: (i) The effective pion-nucleon coupling constant is quenched in the medium, and (ii) the pion-nucleon threshold of the effective amplitude is moved upwards in energy. Both effects are due to Pauli-principle restrictions on nucleons in intermediate states. Like its free-space counterpart, $f(kq;kq)$ displays a resonance behavior in the (3,3) pion-nucleon channel. The resonance appears as a characteristic energy dependence in the pion-nucleus optical potential calculated from $f(kq;kq)$. The resonance position in pion-nucleus scattering is determined by three competing effects, and generally differs from the free pion-nucleon (3,3) resonance energy. One finds that: (i) The quenching effect moves the (3,3) resonance up in energy and narrows its width, (ii) the dispersive effect of the nuclear medium (increase of the real part of the wave number over the free-space value) moves the resonance downward, (iii) the energy dependence of the effective radius $R+\lambda\!\!\!^{-}$ seen by a pion of wavelength $\lambda\!\!\!^{-}$ also shifts the resonance downward in energy. The net energy shift is thus a result of a rather delicate cancellation of several competing effects. Absorption cross sections for negative pions are calculated for a range of nuclei. In general, the net downward energy shift with respect to the free (3,3) resonance is found to increase with increasing mass number.

I. INTRODUCTION

Several recent experiments have been reported on pion scattering from nuclei in the (3, 3) resonance region of pion-nucleon (πN) scattering.[1-4] It is clear from these experiments that there is a close relation between the basic πN (3, 3) resonance[5-8] and the resonance seen in pion-nucleus scattering, except that the latter resonance is shifted downwards with respect to the free πN resonance. In the case of $\pi^- + {}^{12}C$ scattering, for example,[1] the downward shift is about 30 MeV.

There is as yet no systematic experimental evidence for this downward shift for a wide range of nuclei, although such an effect is to be anticipated if one is to believe the philosophy of existing calculations for the resonance shift in $\pi^- + {}^{12}C$ scattering. Several model approaches have been tried in this case.[9-19] These include Glauber theory, multiple-scattering theory, and optical-model calculations. Some of these calculations do predict a downward shift in the resonance of approximately the correct magnitude, but they are all essentially numerical in nature. In spite of some recent attempts in this direction,[19-22] the physical effects which contribute to the energy shift remain somewhat obscure.

The present work attempts to identify and analyze as clearly as possible the various physical processes which enter the pion-nucleus resonance phenomenon. We isolate and discuss three main effects: (i) the quenching of the free-space pion-nucleon interaction by the nuclear medium. This effect generally weakens the effective pion-nucleon coupling in the medium and tends to shift the (3, 3) resonance *upward* in energy. (ii) the dispersion effect of the nuclear medium. This is the nuclear-matter analog of the multiple-scattering effect obtained by solving the Klein-Gordon equation in coordinate space.[19] This effect is found to produce a *downward* shift of the (3, 3) resonance. (iii) the energy-dependence of the effective nuclear radius seen by the incident pion. This effect also produces a *downward* shift.

Each of these three effects turn out to be about equally important; (i) tending to cancel the effects of (ii) and (iii). Thus the actual resonance position in a given nucleus is determined by a rather

delicate interplay of effects (i) to (iii).

Our approach treats the nucleus as a slab of nuclear matter, and is most conveniently couched in the language of propagators.[23,24] The effect of the nuclear medium on a pion propagating through it is fully accounted for in terms of the pion self-energy function $\Pi(q)$, where q is the momentum-energy index $\{\vec{q}, \omega\}$ of the pion.[25,26] We calculate the change of wave number of the pion entering the nuclear medium from $\Pi(q)$. This is conveniently done via a nuclear "refractive index"

$$n^2(\omega) - 1 = \frac{\Pi(\vec{q}, \omega)}{p^2} \tag{1.1}$$

for pions, where p is the incident momentum of a pion with energy ω, so that $q = n(\omega)p$. Since the self-energy $\Pi(q)$ is complex due to pion absorption, so is $n(\omega)$. Thus we can calculate a pion mean free path λ in the medium from the imaginary part of $n(\omega)$, and hence the pion-absorption cross section from λ via the optical model.

Our main effort is directed towards obtaining the pion self-energy $\Pi(q)$. The starting point of our calculation is the observation that the functional derivative of $\Pi(q)$ with respect to a nucleon propagator $G(k)$ (the "cutting" of a nucleon line in graph language) defines an effective forward-scattering amplitude $f(kq; kq)$ for pion-nucleon scattering *in the nuclear medium*. In symbols,

$$\frac{\delta\Pi(q)}{\delta G(k)} = 4\pi i f(kq; kq)\,. \tag{1.2}$$

The zero density limit of Eq. (1.2) yields the usual free-space amplitude $f_0(kq; kq)$ for πN scattering. In the limit of infinitely massive nucleons (the static limit), one knows that $f_0(kq; kq)$ satisfies a Chew-Low equation.[27]

At finite nuclear densities, we find that $f(kq; kq)$ satisfies the modified Chew-Low equation (3.17), provided that we neglect polarization processes induced by the intermediate-state pion. This equation is identical in structure with the free-space Chew-Low equation (3.3), except that the free-space nucleon propagator $G_0(k+q-p)$ in intermediate states in Eq. (3.3) has been replaced by the nucleon propagator $G(k+q-p)$ of a nucleon in the nuclear medium in Eq. (3.17). Ignoring nucleon-nucleon interactions for the moment, one sees that $G(k+q-p)$ registers the effect of the Pauli principle in intermediate pion-nucleon states. The nucleon cannot recoil into occupied states of the Fermi sea, and hence the phase space available to such πN encounters is reduced. This is the physical origin of the quenching effect referred to under item (i). This effect is seen most transparently via Eq. (3.84), which shows how the πN coupling strength λ is modified at threshold to λ', where

$$\lambda' = \frac{\lambda}{(1+4\pi N_0 C)^2}\,, \quad \omega \simeq \mu \tag{1.3}$$

(μ is the pion mass). Here C is the πN scattering volume per scatterer and N_0 the density of scatterers. For $C > 0$, the effective πN coupling constant is *reduced* in the medium.

An important feature of Eq. (1.1) is that it involves $\Pi(\vec{q}, \omega)$ at a pion momentum $\vec{q}$ and energy ω, such that $\omega \neq (q^2+\mu^2)^{1/2}$. This means that the pion propagates "off the energy shell" in the nuclear medium, and we thus require off-shell values of the scattering amplitude $f(kq; kq)$ in order to construct $\Pi(\vec{q}, \omega)$ (by functional integration). It is an added advantage of the present approach that the modified Chew-Low equation (3.17) for $f(kq; kq)$ is valid both on and off the pion energy shell.

A knowledge of $\Pi(\vec{q}, \omega)$ determines $n(\omega)$ at a given incident pion energy ω. Since the πN interaction is pseudoscalar, one finds approximately that $\Pi(\vec{q}, \omega) = q^2\alpha(\omega)$ and thus $n(\omega)$ exhibits a resonance form

$$n^2(\omega) - 1 = \frac{\alpha(\omega)}{1-\alpha(\omega)} \tag{1.4}$$

that describes the dispersion and absorption of the pion wave in close analogy with the scattering of a light wave by a classical medium.[28] In the case of pion-nucleus scattering, one finds that the dispersion tends to move the (3, 3) resonance *downward* in energy.

The general outline of the paper is as follows: In Sec. II we introduce the necessary formalism to define the pion self-energy, refractive index, and pion mean free path in the nuclear medium. Section III reviews the standard Chew-Low theory for free πN scattering in a nonstandard way, making use of graphs to derive the nonlinear integral equation for the scattering amplitude. The discussion is then extended to include scattering from nucleons in a nuclear medium, and a rather complete discussion of the properties of this amplitude is presented, with particular reference to the quenching effect of the medium. Section IV presents numerical solutions of the modified Chew-Low equation for a variety of nuclei from ^{4}He to ^{208}Pb. We give predictions of the (3, 3) resonance energy as a function of mass number A. The summary, conclusions, and criticisms are to be found in Sec. V.

II. PROPAGATION OF PIONS IN THE NUCLEAR MEDIUM

The language of propagators, or Green's functions, is used for the present discussion.[23-26] Since we will be discussing pions propagating in

a nuclear medium of infinite extent, it is useful to introduce a plane-wave basis in which meson and nucleon states are labeled by their three-momenta $\vec{p}$, $\vec{k}$, etc., together with the spin and isospin labels $\{\sigma, \tau\}$ for nucleons and a single isospin label $\{\alpha\}$ for the spinless pions. We normalize all plane-wave states in a box of unit volume and choose units such that $\hbar = c = 1$.

We now introduce the basic time-ordered propagators that are required in the theoretical developments to follow. These are (i) the single-pion propagator defined by

$$D(\vec{q}\alpha, t) = i\langle T\{Q_{\vec{q}\alpha}(t) Q^{\dagger}_{\vec{q}\alpha}(0)\}\rangle \tag{2.1}$$

for a pion of momentum $\vec{q}$ and isospin index α, and (ii) the single-nucleon propagator defined by

$$G(\vec{p}\nu, t) = i\langle T\{a_{\vec{p}\nu}(t) a^{\dagger}_{\vec{p}\nu}(0)\}\rangle \tag{2.2}$$

for a nucleon of momentum $\vec{p}$ and spin-isospin index $\nu = \{\sigma, \tau\}$. In Eq. (2.2), the $a^{\dagger}_{\vec{p}\nu}$ and $a_{\vec{p}\nu}$ are the usual creation and destruction operators for a nucleon in state $\{p, \nu\}$ with energy $\epsilon_{\vec{p}} = p^2/2m$ (m is the nucleon mass). The operators appearing in Eq. Eq. (2.1) are defined by

$$Q_{\vec{q}\alpha} = (2\omega_{\vec{q}\alpha})^{-1/2}(B_{\vec{q}\alpha} + B^{\dagger}_{-\vec{q}\alpha}) \tag{2.3}$$

(together with the Hermitian conjugate of this equation) in terms of creation and destruction operators $B^{\dagger}_{\vec{q}\alpha}$ and $B_{\vec{q}\alpha}$ of pions in the state $\{\vec{q}, \alpha\}$ having a total energy $\omega_{\vec{q}\alpha} = (\mu^2 + q^2)^{1/2}$, where μ is the rest mass of the pion. The symbol T in Eqs. (2.1) and (2.2) denotes the chronological time-ordering operator. The angular brackets indicate that the expectation value of the resultant product is formed with respect to the exact ground state of the coupled pion-nucleus system.

We will also require the Fourier transforms of D and G. These are defined by the equations

$$\begin{aligned} D(\vec{q}\alpha, \omega) &= \int_{-\infty}^{+\infty} dt\, e^{i\omega t} D(\vec{q}\alpha, t), \\ G(\vec{p}\nu, \epsilon) &= \int_{-\infty}^{+\infty} dt\, e^{i\epsilon t} G(\vec{p}\nu, t). \end{aligned} \tag{2.4}$$

The propagators for a free pion or nucleon are elementary,[23-26] and their corresponding Fourier transforms are given by

$$D_0(\vec{q}, \omega) = \frac{1}{(\omega_{\vec{q}} - i\delta)^2 - \omega^2} \tag{2.5}$$

and

$$G_0(\vec{p}, \epsilon) = \frac{1}{\epsilon_{\vec{p}} - \epsilon - i\delta}. \tag{2.6}$$

The positive infinitesimal δ locates the poles of these functions appropriately.[24] Note that the free propagators D_0 and G_0 are taken to be independent of the spin and/or isospin of the particles.

We now introduce the self-energy $\Pi(q)$ of a pion propagating in the nuclear medium according to the equation

$$D(q) = D_0(q) + D_0(q)\,\Pi(q) D(q), \tag{2.7}$$

where $q = \{\vec{q}, \omega\}$. In the language of Feynman diagrams, $\Pi(q)$ is given by the sum of all irreducible diagrams having two external pion legs.[23,24] The energy-momentum relation of a pion propagating in the nuclear medium is given by the pole of $D(q)$. Rewriting Eq. (2.7) in the form

$$D(q) = \frac{1}{\omega_{\vec{q}}^2 - \omega^2 - \Pi(q)}, \tag{2.8}$$

we see that the pion energy-momentum relation is

$$\omega^2 = \omega_{\vec{q}}^2 - \Pi(\vec{q}, \omega) = q^2 + \mu^2 - \Pi(\vec{q}, \omega), \tag{2.9}$$

instead of $\omega = \omega_{\vec{q}}$, as in free space. Thus a pion of momentum $\vec{q}$ propagates off its energy shell in the nuclear medium. In Eq. (2.9) we are free to fix either the pion energy ω or the pion momentum $\vec{q}$. In the present instance, we are interested in how pions of a prescribed energy propagate in the nuclear medium. Thus ω is fixed by $\omega = (p^2 + \mu^2)^{1/2}$, where $\vec{p}$ is the momentum of the incident pion in free space and we determine $\vec{q}$ from Eq. (2.9). The energy ω is of course the same for the pion both inside and outside the nucleus, the interaction with the nuclear medium bringing about the change in the momentum of the pion.

As in classical optics, it is therefore useful to characterize the medium by a refractive index n,

$$n(\omega) = q/p. \tag{2.10}$$

In our case $n(\omega)$ is found by solving Eq. (2.9) for the ratio q/p after stipulating that $\omega = (p^2 + \mu^2)^{1/2}$. One finds that

$$n^2(\omega) - 1 = (1/p^2)\Pi(\vec{q}, \omega). \tag{2.11}$$

Equation (2.11) is *exact*. However, it requires a knowledge of how $\Pi(\vec{q}, \omega)$ depends on $\vec{q}$ and ω separately. Thus we must have a model for calculating $\Pi(q)$ that details these separate dependences. This point is discussed in detail in Sec. III.

As in classical optics, we can pass from a knowledge of $n(\omega)$ to the mean free path λ of pions in nuclear matter by evaluating the imaginary part of $n(\omega)$:

$$1/\lambda = 2p\,\mathrm{Im} n(\omega). \tag{2.12}$$

This equation will allow us to estimate the absorption cross section of pions by various nuclei in the optical limit.

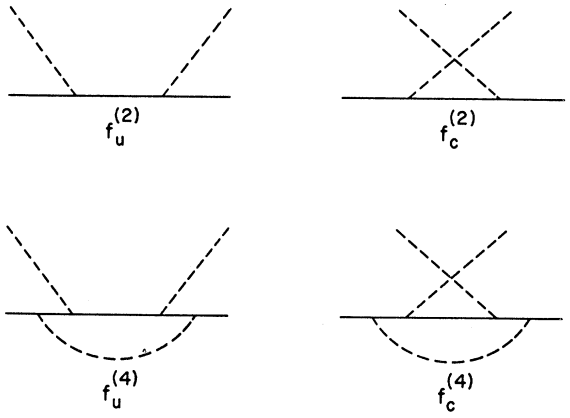

FIG. 1. Irreducible pion-nucleon scattering graphs to second and fourth order in the coupling constant f_r. The dashed lines represent pions while the solid line indicates the nucleon. We have introduced the notation $f_u^{(2)}$ = second-order graph with uncrossed external lines, $f_c^{(2)}$ = second order with crossed lines, etc.

III. EFFECTIVE PION-NUCLEON INTERACTION IN THE MEDIUM

A. Review of the Chew-Low Theory— An Alternative Derivation

We first review the usual Chew-Low theory[27] of pion-nucleon scattering. We do so by presenting a graphical derivation of the Chew-Low equation, which makes rather transparent its extension to pion scattering from a nucleon in a nucleus.

Using the language of Feynman diagrams, let us consider all *irreducible* graphs for pion-nucleon scattering in each order of perturbation theory in the pion-nucleon coupling constant f_r. (We use the rationalized, renormalized value of f_r throughout this paper, which means that $f_r^2/4\pi = 0.08$.) These graphs are shown in Figs. 1 and 2 through order f_r^6. The remaining pion-nucleon graphs that one can draw to the same order are *reducible* in the sense that they either renormalize the coupling

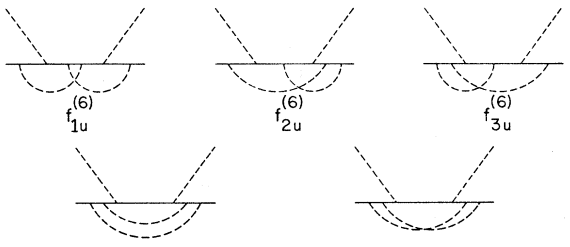

FIG. 2. Sixth-order irreducible pion-nucleon scattering graphs. We have not shown the counterpart of each graph with crossed external lines. The last two graphs, which involve two-pion intermediate states, are not included in the Chew-Low equation.

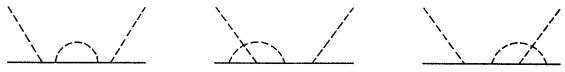

FIG. 3. Fourth-order reducible pion-nucleon graphs. The first process represents a self-energy insertion, and is already included in the definition of the dressed nucleon. The second and third processes are vertex renormalizations, and are included in the definition of the renormalized coupling constant.

constant (vertex renormalization) or "dress" the nucleon propagator (self-energy insertions). In Fig. 3 we show typical reducible graphs to order f_r^4.

In order to derive the Chew-Low equation for the pion-nucleon scattering amplitude, we first introduce an amplitude $4\pi i f(kq; k'q')$, see Fig. 4, labeled by the four-momenta $k = \{\vec{k}, k_0\}$ and $q = \{\vec{q}, q_0\}$ of the nucleon and the pion in the initial state; k' and q' are the same quantities in the final state. The amplitude $f(kq; k'q')$ thus defined only becomes the *physical* scattering amplitude when both the pion and the nucleon lines are "on shell," i.e., $q_0 = \omega_{\vec{q}} = (q^2 + \mu^2)^{1/2}$ and $k_0 = \epsilon_{\vec{k}} = k^2/2m$ etc., in the initial and the final states. The normalization of f is such that $|f|^2$ gives the cross section for prescribed initial and final states without additional factors.

Consider the product[29] $f^\dagger f$ after formally expanding f in terms of the perturbation series of *irreducible* graphs shown in Figs. 1 and 2. One can perform the conjunction $f^\dagger f$ graphically by imagining two irreducible graphs side by side and then connecting the nucleon line and one pair of pion lines. Typical conjunctions are shown in Fig. 5. For any given pair of graphs, the pion lines can be connected in two, rather than four different ways since we must remain with one incoming and one outgoing pion. Thus each conjunction leads to two graphs in the next order. One of these is reducible, the other not. We reject the reducible graphs as explained above. The irreducible conjunctions of $f^\dagger f$ are then found to generate the set of graphs (apart from the Born term) for the amplitude f which only have *one* pion in intermediate states for at least part of the time. For example, the last two graphs of Fig. 2 are *not* generated by $f^\dagger f$. We return to this point again.

To illustrate the procedure outlined above, introduce the notation $f_u^{(2i)}$ and $f_c^{(2i)}$ for the irreducible graphs with uncrossed and crossed external pion lines that contribute to f in order $i = 1, 2, \ldots$. Then one sees for example that $f^{(2)\dagger} f^{(2)}$ generates $f^{(4)}$ according to

$$f_u^{(2)\dagger} f_u^{(2)} \to f_c^{(4)}, \qquad f_c^{(2)\dagger} f_c^{(2)} \to f_u^{(4)}. \tag{3.1}$$

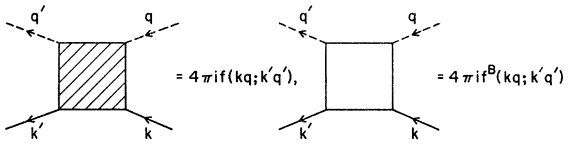

FIG. 4. Pictorial representation of the pion-nucleon scattering amplitude $f(kq;\, k'q')$. The incoming nucleon and pion lines are labeled by four-momenta $k=\{\vec{k}, k_0\}$ and $q=\{\vec{q}, q_0\}$, respectively. The amplitude f is related to the amplitude T defined by Chew and Low (Ref. 27) $f(kq;kq)=-\omega_{\vec{q}}T_q(q)/2\pi$. Our f has the property that the differential cross section $d\sigma/d\Omega$ for the pion-nucleon scattering is given by $d\sigma/d\Omega=|f|^2$.

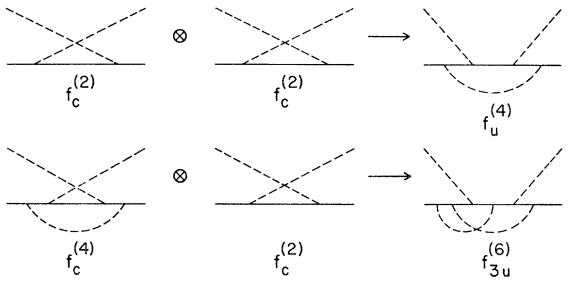

FIG. 5. Pictorial multiplication of graphs in the perturbation series for f. To get the product shown on the right, one connects one pair of pion lines, and the nucleon lines. The product graph is another irreducible graph in the perturbation series.

In the next order one finds (Fig. 2 identifies the individual graphs)

$$\begin{aligned} &f_c^{(2)\dagger}f_u^{(4)}\to f_{1u}^{(6)},\\ &f_u^{(2)\dagger}f_c^{(4)}\to f_{1c}^{(6)},\\ &f_c^{(2)\dagger}f_c^{(4)}\to f_{2u}^{(6)},\\ &f_u^{(2)\dagger}f_u^{(4)}\to f_{2c}^{(6)}, \end{aligned} \tag{3.2}$$

with corresponding results for $f^{(4)\dagger}f^{(2)}$. One observes that the graph corresponding to $f_{1u}^{(6)}$ (and its crossed version) is left-right symmetric. Consequently it will formally be generated twice, once from $f_c^{(2)\dagger}f_u^{(4)}$ and once from $f_u^{(4)\dagger}f_c^{(2)}$. Both of these conjunctions correspond to the *same* graph of course and only one is to be taken in the *graphical* expansion of f. The fact that this counting procedure reproduces the Chew-Low equation confirms that it is correct.

We have thus shown that, apart from the two lowest-order Born graphs $f_u^{(2)}$ and $f_c^{(2)}$ of Fig. 1, the conjunction $f^\dagger f$ generates *all* graphs for f that we consider. The summation of these graphs can thus be accomplished by "solving" the graphical equation shown in Fig. 6 for the cross-hatched box diagram that represents $4\pi if$. In Fig. 6, the unhatched box represents the Born approximation $4\pi if^B$, given by the sum of graphs $f_u^{(2)}+f_c^{(2)}$ shown in Fig. 1. Upon supplying the propagators iG_0 and iD_0 for the intermediate-state nucleons (solid lines) and pions (dashed lines), the graphical equation of Fig. 6 translates into the following *nonlinear* integral equation for the amplitude f. After passing to integrals to symbolize the sum over *all* intermediate-state variables p, one has

$$\begin{aligned} f(kq;\, k'q') = f^B(kq;\, k'q') &- 4\pi i\int \frac{d^4p}{(2\pi)^4}\, D_0(p)G_0(k+q-p)f^\dagger(k'q';\, k+q-p,p)f(kq;\, k+q-p,p)\\ &- 4\pi i\int \frac{d^4p}{(2\pi)^4}\, D_0(p)G_0(k-q'-p)f^\dagger(k',-q;\, k-q'-p,p)f(k,-q';\, k-q'-p,p)\,, \end{aligned} \tag{3.3}$$

upon canceling a common factor $4\pi i$. The conservation of four-momentum requires $k+q=k'+q'$ in Eq. (3.3). We emphasize that this equation for f includes *all* graphs containing one virtual pion in the intermediate state, but *none* of the graphs containing two or more virtual pions which are present for the *entire* time between absorption and emission of the external pion. Graphs in which two or more pions are present for part but not all of the time *are* included (examples being $f_{1u}^{(6)}$, $f_{2u}^{(6)}$, and $f_{3u}^{(6)}$ in Fig. 2). The last term (the crossing term) in Eq. (3.3) ensures that f is crossing symmetric.[27] It is obtained from the term with uncrossed pion lines by the transformation $(q\leftrightarrow -q')$.

We now demonstrate that Eq. (3.3) reduces to the Chew-Low equation[27] in the static limit $\mu/m\to 0$, where m is the nucleon mass. An equivalent statement of the static limit is that the amplitudes f in Eq. (3.3) cannot depend on the nucleon four-momentum variables, but only their spin and isospin. Then we may perform the integral over the nucleon intermediate-energy variable $k_0+q_0-p_0$ (or equivalently p_0) by contour integration to find

$$\begin{aligned} \int \frac{dp_0}{2\pi}\, D_0(p)G_0(k+q-p)f^\dagger(k'q';\, k+q-p,p)f(kq;\, k+q-p,p) &= \frac{i}{2\omega_{\vec{p}}}\,\frac{[f^\dagger(q',p)f(q,p)]_{p_0=\omega_{\vec{p}}}}{\epsilon_{\vec{k}+\vec{q}-\vec{p}}-\epsilon_{\vec{k}}-q_0+\omega_{\vec{p}}-i\delta}\\ &\simeq \frac{i}{2\omega_{\vec{p}}}\,\frac{[f^\dagger(q',p)f(q,p)]_{p_0=\omega_{\vec{p}}}}{\omega_{\vec{p}}-q_0-i\delta} \end{aligned} \tag{3.4}$$

after neglecting all nucleon energies in the final step in accord with the static limit condition. Hence $q_0 = q_0'$. In Eq. (3.4) we have set $f(kq; k+q-p, p) \equiv f(q, p)$ to emphasize the dependence on the pion four-momenta only. The result (3.4) is only consistent in the external variables q and q' if $q_0 = q_0'$. This is so because the general four-momenta conservation law $k+q = k'+q'$ leads one to conclude that

$$q_0 - q_0' = (\epsilon_{\vec{k}}' - \epsilon_{\vec{k}}) \simeq 0$$

in the static limit (here we consider the external nucleons to be on shell). Therefore, the amplitude $f(q, q')$ is more conveniently written as $f(\vec{q}, \vec{q}'; \omega)$ where ω is an energy parameter (note that $\vec{q} \neq \vec{q}$ in general, since static nucleons can accept any amount of momentum). In general, $f(\vec{q}, \vec{q}'; \omega)$ is a fully off-shell amplitude; its half-off-shell value $f(\vec{q}, \vec{p}, \omega_{\vec{p}})$ appears in Eq. (3.4), while if $\omega = \omega_{\vec{q}} = \omega_{\vec{q}'}$ the resulting amplitude $f(\vec{q}, \vec{q}', \omega_{\vec{q}})$ is the on-shell physical scattering amplitude. Bearing these remarks in mind, we use Eq. (3.4) and its crossed version under the exchange $\{\vec{q} \to \vec{q}', \omega \to -\omega\}$ to obtain

$$f(\vec{q}, \vec{q}'; \omega) = f^B(\vec{q}, \vec{q}', \omega) + 2\pi \int \frac{d^3\vec{p}}{(2\pi)^3} \frac{1}{\omega_{\vec{p}}} \left(\frac{f^\dagger(\vec{q}', \vec{p}; \omega_{\vec{p}}) f(\vec{q}, \vec{p}; \omega_{\vec{p}})}{\omega_{\vec{p}} - \omega - i\delta} + \frac{f^\dagger(-\vec{q}, \vec{p}; \omega_{\vec{p}}) f(-\vec{q}', \vec{p}; \omega_{\vec{p}})}{\omega_{\vec{p}} + \omega - i\delta} \right), \tag{3.5}$$

in place of Eq. (3.3). This equation expresses the off-shell amplitude $f(\vec{q}, \vec{q}'; \omega)$ in terms of the half-off-shell amplitudes $f(\vec{q}, \vec{p}; \omega_{\vec{p}})$.

When $\omega = \omega_{\vec{q}} = \omega_{\vec{q}'}$, i.e., when the external pions are on shell, Eq. (3.5) is just the Chew-Low equation, if we assume a pseudoscalar pion-nucleon coupling. To see this in detail, we recall that in the static limit the dependence of $f(\vec{q}, \vec{q}'; \omega)$ on $\vec{q}$ and $\vec{q}'$ for pseudoscalar mesons is known trivally since only p-wave scattering occurs. We exhibit this property by means of projection operators $P_\alpha(\vec{q}', \vec{q})$ onto the four allowed isospin-spin channels $\alpha = \{2T, 2J\} = \{11, 13, 31, 33\}$ and set

$$f(\vec{q}, \vec{q}'; \omega) = \sum_\alpha P_\alpha(\vec{q}', \vec{q}) \overset{0}{h}_\alpha(\omega), \tag{3.6}$$

where the superscript zero on $\overset{0}{h}$ will serve as a reminder that Eq. (3.6) refers to scattering from an isolated nucleon (the zero-density case). Explicit forms for the $P_\alpha(\vec{q}', \vec{q})$ have been written down by Chew and Low[27]:

$$\begin{aligned} P_{11}(\vec{q}', \vec{q}) &= \tfrac{1}{3} \tau_r' \tau_r (\vec{\sigma} \cdot \vec{q}')(\vec{\sigma} \cdot \vec{q}), \\ P_{13}(\vec{q}', \vec{q}) &= \tfrac{1}{3} \tau_r' \tau_r [3(\vec{\sigma} \cdot \vec{q}')(\vec{\sigma} \cdot \vec{q}) - (\vec{\sigma} \cdot \vec{q}')(\vec{\sigma} \cdot \vec{q})], \\ P_{31}(\vec{q}', \vec{q}) &= (\delta_{r'r} - \tfrac{1}{3} \tau_r' \tau_r)(\vec{\sigma} \cdot \vec{q}')(\vec{\sigma} \cdot \vec{q}), \\ P_{33}(\vec{q}', \vec{q}) &= (\delta_{r'r} - \tfrac{1}{3} \tau_r' \tau_r)[3(\vec{\sigma} \cdot \vec{q}')(\vec{\sigma} \cdot \vec{q}) - (\vec{\sigma} \cdot \vec{q}')(\vec{\sigma} \cdot \vec{q})]. \end{aligned} \tag{3.7}$$

Note that we have absorbed the coordinate $r = 1, 2, 3$ relating to the three charge states of the pion into the symbol $\vec{q}$ etc. on the left-hand side of Eq. (3.7), a practice we shall continue to follow. The operators $\vec{\sigma}$ and $\vec{\tau}$ refer to the spin and isospin of an isolated nucleon. We also remark that the expansion (3.6) is not useful if we attempt to include nucleon recoil (albeit without any real justification) in Eq. (3.5). Instead a complete partial-wave expansion would have to be considered.

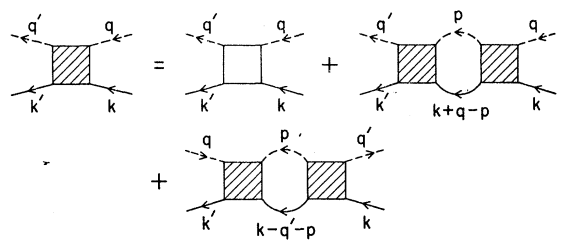

FIG. 6. Graphical representation of the integral equation (3.3) for the pion-nucleon scattering amplitude $f(kq; k'q')$. The last term is the "crossing" amplitude.

We now substitute the expansion (3.6) into Eq. (3.5) for f. The direct term in Eq. (3.5) involves the product of projection operators $P_\alpha P_\beta$. This can be reexpressed as[30]

$$\int d\Omega_{\vec{p}} P_\alpha(\vec{q}', \vec{p}) P_\beta(\vec{p}, \vec{q}) = 4\pi p^2 P_\alpha(\vec{q}', \vec{q}) \delta_{\alpha\beta}, \tag{3.8}$$

where $d\Omega_{\vec{p}}$ is the differential solid angle associated with the vector $\vec{p}$. In the crossing term a projector $P_\beta(-\vec{q}, -\vec{q}') = P_\beta(\vec{q}, \vec{q}')$ appears on the right-hand side of Eq. (3.8) instead. However the crossing relation[27]

$$P_\beta(\vec{q}, \vec{q}') = \sum_\alpha A_{\alpha\beta} P_\alpha(\vec{q}', \vec{q}), \tag{3.9}$$

where $A_{\alpha\beta}$ is the crossing matrix

$$(A_{\alpha\beta}) = \frac{1}{9} \begin{pmatrix} 1 & -4 & -4 & 16 \\ -2 & -1 & 8 & 4 \\ -2 & 8 & -1 & 4 \\ 4 & 2 & 2 & 1 \end{pmatrix} \tag{3.10}$$

allows us to reverse $\vec{q}$ and $\vec{q}'$. Using Eqs. (3.8) and (3.4) in conjunction with the expansion (3.6) for f leads to the following set of coupled equations for the $\overset{0}{h}_\alpha$:

$$\overset{0}{h}_\alpha(\omega) = \frac{\overset{0}{\lambda}_\alpha}{\omega} + \frac{1}{\pi} \int_\mu^\infty d\omega_{\vec{p}}\, p^3 v^2(p) \times \left(\frac{|\overset{0}{h}_\alpha(\omega_{\vec{p}})|^2}{\omega_{\vec{p}} - \omega - i\delta} + \sum_\beta A_{\alpha\beta} \frac{|\overset{0}{h}_\beta(\omega_{\vec{p}})|^2}{\omega_{\vec{p}} + \omega - i\delta} \right). \tag{3.11}$$

The intermediate steps involved in obtaining (3.11) have been to shift from the momentum $\vec{p}$ to the energy $\omega_{\vec{p}} = (p^2+\mu^2)^{1/2}$ of the intermediate pion as integration variable, and to include a nucleon form factor $v^2(p)$ to prevent high momentum divergences due to the use of point nucleons. The coupling constants $\overset{0}{\lambda}_\alpha$ appearing in the Born amplitude λ_α/ω are identified as

$$\lim_{\omega\to 0} \omega \overset{0}{h}{}^{B}_{\alpha}(\omega) = \overset{0}{\lambda}_\alpha = \frac{f_r^{\,2}}{4\pi\mu^2}\frac{2}{3}\begin{pmatrix} -4 \\ -1 \\ -1 \\ 2 \end{pmatrix} \tag{3.12}$$

by computing the Born amplitude,

$$4\pi i f^B(\vec{q},\vec{q}';\omega) = \frac{i f_r^{\,2}}{\mu^2}\{(\vec{\sigma}\cdot\vec{q}')(\vec{\sigma}\cdot\vec{q})\tau_{r'}\tau_r G_0(k+q) + (q\to -q')\}_{q_0=q_0'=\omega} \tag{3.13}$$

in the static limit, $G_0(k\pm q)\simeq \mp(1/q_0)$, and projecting onto states of good $\{J, T\}$. Equation (3.11) is the more familiar form of the Chew-Low equation for pion-nucleon scattering. The form factor $v^2(p)$ is of course arbitrary here, as in the original treatment[27] and is simply a device for ensuring convergence of an otherwise divergent integral. Clearly we expect convergence difficulties, since our approach is nonrelativistic.[27,30] These difficulties will not be discussed here. In later sections we simply adopt a one-parameter form for $v^2(p)$, and adjust this parameter to correctly position the pion-nucleon (3, 3) resonance.

Equation (3.11) gives us a prescription for evaluating the amplitudes $\overset{0}{h}_\alpha(\omega)$ off shell $\omega \neq \omega_{\vec{q}}$. By contrast, Eq. (3.3) allows an extrapolation of $f(kq; k'q')$ in both energy variables q_0 and q_0'. As will be seen, the problem of computing the pion-nucleus self-energy $\Pi(\vec{q},\omega)$ only requires the special case $q_0 = q_0' = \omega \neq \omega_{\vec{q}}$, i.e., an off-shell extrapolation in *one* variable.

The derivation of the Chew-Low equation given here serves two purposes: (a) It provides a straightforward graphical derivation of the Chew-Low equation which can easily be extended (see next section) to the case of pion scattering from nucleons in a nucleus and (b) it leads to a prescription for obtaining the off-shell extension of the Chew-Low amplitudes that confirms the original prescription of Chew and Low.[31]

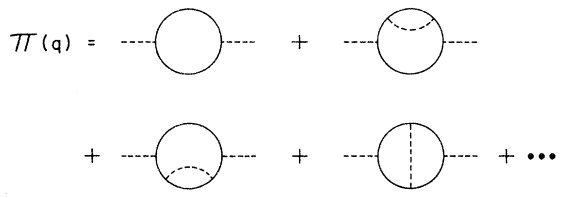

FIG. 7. Simplest perturbation-theory diagrams for the pion self-energy $\Pi(q)$, containing one particle-hole bubble.

B. Pion Scattering from Nucleons in a Nucleus

We now proceed to the problem at hand: How is the Chew-Low equation (3.11) modified by the presence of the nuclear medium? The motivation for this question comes from looking at the connection between the pion self-energy in a nucleus (represented now by nuclear matter) and the free pion-nucleon forward-scattering amplitude f_0. At low densities n_0, one finds

$$\Pi(\vec{q},\omega) \simeq 4\pi n_0 f_0(kq; kq), \tag{3.14}$$

a result that can be derived in many ways. One way[26] is to use the fact that the functional derivative of each self-energy diagram for $\Pi(q)$ with respect to an intermediate nucleon propagator $G_0(p)$ yields a graph which contributes to the pion-nucleon scattering amplitude. Thus, upon summing all such graphs, one has the formal result

$$\frac{\delta\Pi(q)}{\delta G_0(k)} = 4\pi i f_0(kq; kq) \tag{3.15}$$

from which Eq. (3.14) then follows, as is shown in detail in Ref. 26.

If the density of the medium is not small, the situation is more complicated. However, if we

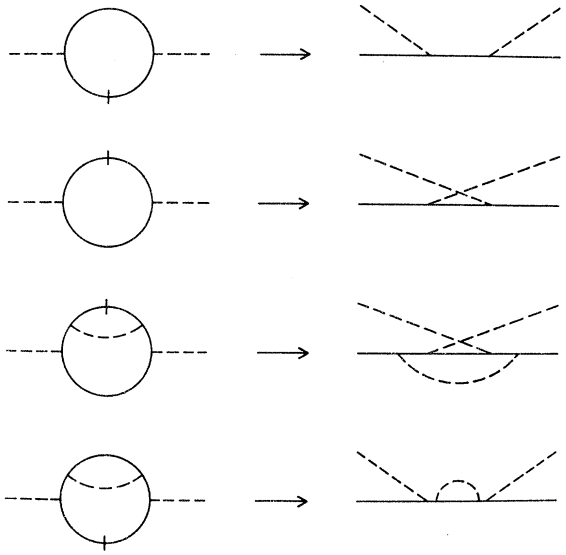

FIG. 8. Illustration of the pion-nucleon scattering graphs which result from cutting a single nucleon line (functional differentiation) in pion self-energy diagrams. The nucleon line that has been cut is cross-hatched. The corresponding cut diagram (unfolded) is shown on the right-hand side.

restrict the diagrams contributing to $\Pi(q)$ to be of the type depicted in Fig. 7, i.e. any number of intermediate pions, but a *single* particle-hole bubble, then a major simplification occurs. For then it is clear that the functional derivative

$$\frac{\delta\Pi(q)}{\delta G(k)} = 4\pi i f(kq; kq), \tag{3.16}$$

where $G(k)$ refers to a renormalized nucleon propagator in the medium (see below), *defines* a density-dependent effective πN forward-scattering amplitude $f(kq; kq)$ in the medium. The amplitude $f(kq; kq)$ is given by exactly the same set of graphs as $f_0(kq; kq)$, but with G replacing the free-nucleon Green's function G_0 everywhere. The nucleon described by G carries self-energy insertions due to meson exchange with the *inert* nuclear medium (Hartree-Fock insertions) in addition to mass renormalizations due to interactions with its own meson field.

In graphical language, a functional derivative like $\delta/\delta G$ corresponds to cutting each nucleon line in turn in each graph for $\Pi(q)$. The result is a graph with two external nucleon lines as well as two external pion lines. This cutting process is shown pictorially in Fig. 8 for some of the graphs for $\Pi(q)$. The graphs generated in this way can again be grouped into the three classes: nucleon self-energy insertions, vertex renormalizations, and irreducible graphs that contribute to $f(kq; kq)$. As previously, we absorb the self-energy insertions and vertex renormalizations into the renormalized nucleon propagator and pion-nucleon coupling constant. Note that these renormalizations are now *density-dependent*. In particular, the renormalized πN coupling constant need *not* equal the free one f_r used in Eq. (3.13).

The remaining irreducible graphs can now be summed as before to yield an integral equation for $f(kq; kq)$. Considering for the moment the more general amplitude $f(kq; k'q')$, where $k+q = k'+q'$ as before, one has

$$\begin{aligned} f(kq; k'q') = {} & f^B(kq; k'q') \\ & - 4\pi i\Big[\int \frac{d^4p}{(2\pi)^4} D_0(p) G(k+q-p) \\ & \times f^\dagger(k'q'; k+q-p, p) f(kq; k+q-p, p) \\ & + (q \to -q')\Big]. \end{aligned} \tag{3.17}$$

The renormalized coupling constant enters this equation via the Born amplitude f^B, and also partially via the propagator G that carries the self-energy insertions. A part of these insertions are due to the pion-nucleon interactions [which correspond to the one-pion-exchange part of the nucleon-nucleon interaction] but nucleon-nucleon interactions that do not arise from simple pion exchange also contribute to G. Note also that the free pion propagator D_0 must appear in Eq. (3.17). This is so because of our restriction on the category of graphs we consider. Renormalization of the pion lines would involve multiple particle-hole pairs in intermediate states, contrary to our assumptions.

On the other hand, the nucleon propagator G is renormalized, as outlined in the previous paragraph. Symbolically, we may write

$$G(p) = G_0(p) + G_0(p)\sum(p)G(p), \tag{3.18}$$

where $\sum(p)$ is the self-energy insertion referred to previously. Thus G differs from G_0 due to the effects of the medium on nucleon propagation through it. In the simplest case these are just Pauli-principle effects, interactions being excluded. For example, treating the nucleons as an assembly of noninteracting fermions (i.e. an ideal Fermi gas), one has[23,24]

$$\begin{aligned} G(p) &= G(\vec{p}, p_0) \\ &= \left(\frac{n(\vec{p})}{\epsilon_{\vec{p}} - p_0 + i\delta} + \frac{1-n(\vec{p})}{\epsilon_{\vec{p}} - p_0 - i\delta}\right), \end{aligned} \tag{3.19}$$

where $\delta \to 0^+$ as before, and $n(\vec{p})$ is the occupation number of the state $\vec{p}$ in a Fermi gas, being one or zero according to $|\vec{p}| \lesssim p_F$, where p_F is the Fermi momentum. For $p_F \to 0$, Eq. (3.19) reduces to the free propagator (2.6), while for finite p_F it correctly registers the effect of the Pauli principle. Later in this section we discuss further modifications of G (Hartree-Fock corrections). For later use we also that Eq. (3.19) can be written as

$$G_0(p) - G(p) = 2\pi i n(\vec{p})\delta(\epsilon_{\vec{p}} - p_0) \tag{3.20}$$

so that G_0 and G only differ on the energy shell in a Fermi gas. In particular, this shows that the Born term f^B is *not* modified by self-energy insertions in a Fermi gas. Therefore f_0^B and f^B can differ only in coupling constant due to the density-dependent vertex renormalization in f^B.

We now come to the basic point of our method. By excluding certain multiple particle-hole excitations from the diagrams that contribute to $\Pi(q)$ we have isolated a subset of diagrams for which we can perform the sum to infinity, not of the subset itself, but its functional derivative. This summation is accomplished by Eq. (3.17). In principle one can then obtain $\Pi(q)$ by solving Eq. (3.16), i.e. by performing a functional integration. In general this would be a very complicated procedure. However, in the Fermi-gas model, one can reexpress Eq. (3.16) in terms of the functional derivative of $\Pi(q)$ with respect to the occupation

numbers $n(\vec{k})$:

$$\frac{\delta\Pi(q)}{\delta n(\vec{k})} = \int \frac{d^4p}{(2\pi)^4} \frac{\delta\Pi(q)}{\delta G(p)} \frac{\delta G(p)}{\delta n(\vec{k})} = 4\pi f(kq; kq)|_{k_0=\epsilon_{\vec{k}}} \tag{3.21}$$

after computing

$$\frac{\delta G(p)}{\delta n(\vec{k})} = -i(2\pi)^4 n(\vec{p})\delta(\vec{p}-\vec{k})\delta(p_0-\epsilon_{\vec{p}}) . \tag{3.22}$$

Furthermore, if $f(kq; kq)$ turns out to depend on the occupation numbers $n(\vec{k})$ only through the total density $n_0 = \sum_{\vec{k}} n(\vec{k})$, the functional integration of Eq. (3.16) is equivalent to an ordinary integration over the total density variable. Hence[32]

$$\Pi(q) = 4\pi \int_0^{n_0} dn_0' f(q, n_0') , \tag{3.23}$$

where we write $f(q, n_0')$ to emphasize the density dependence of f. In Eq. (3.23), we integrate over all values of n_0' up to the actual nuclear density n_0. The connection (3.16) between $\Pi(q)$ and the effective density-dependent scattering amplitude f forms the basis of our later discussion of the pion-nucleus optical potential. As a check, note that Eq. (3.23) correctly reduces to the low-density result (3.14) if we replace f by the free pion-nucleon amplitude f_0 and then integrate on n_0'.

The next task is to calculate the effective amplitude f in a medium of prescribed density n_0. We can reduce Eq. (3.17) in the Fermi-gas case by inserting for G the expression (3.20). The integrand $D_0 G f^\dagger f$ then splits into $D_0 G_0 f^\dagger f$, plus a remainder in which the *nucleon* is placed on shell[33] [by the δ function in Eq. (3.20)]. The part with G_0 is *identical* in form with the free-space Chew-Low equation and can be treated as before. For the "remainder," one finds

$$-4\pi \int \frac{d^3\vec{p}}{(2\pi)^3} n(\vec{k}+\vec{q}-\vec{p}) [D_0(p) f^\dagger(k'q'; k+q-p, p) f(kq; k+q-p, p)]_{p_0=k_0+q_0-\epsilon_{\vec{k}+\vec{q}}} \simeq -4\pi \int \frac{d^3\vec{p}}{(2\pi)^3} n(\vec{q}-\vec{p}) \frac{[f^\dagger(q', p) f(q, p)]_{p_0=q_0}}{(\omega_{\vec{p}} - i\delta)^2 - q_0^2} \tag{3.24}$$

in the static limit, i.e. after setting $\vec{k}=0$ and neglecting all intermediate nucleon energies. Note, however, that the nucleon line $k+q-p$ is always on shell in our approximation. As before, we observe that $q_0 = q_0'$. Introducing the notation $f(\vec{q}, \vec{q}'; \omega)$ with $q_0 = \omega$, for the static limit of f, we now gather together the various terms contributing to Eq. (3.17):

$$f(\vec{q}, \vec{q}'; \omega) = f^B(\vec{q}, \vec{q}'; \omega) + \left\{ \int \frac{d^3\vec{p}}{(2\pi)^3} \left[\frac{2\pi}{\omega_{\vec{p}}} \frac{f^\dagger(\vec{q}', \vec{p}; \omega_{\vec{p}}) f(\vec{q}, \vec{p}; \omega_{\vec{p}})}{\omega_{\vec{p}} - \omega - i\delta} - 4\pi n(\vec{q}-\vec{p}) \frac{f^\dagger(\vec{q}', \vec{p}; \omega) f(\vec{q}, \vec{p}; \omega)}{(\omega_{\vec{p}} - i\delta)^2 - \omega^2} \right] + (\vec{q} \to -\vec{q}', \omega \to -\omega) \right\} . \tag{3.25}$$

The additional terms characterized by $\{\vec{q} \to -\vec{q}', \omega \to -\omega\}$ come from crossing symmetry, as for Eq. (3.5).

The first two terms of Eq. (3.25) are identical in form to Eq. (3.5). The third term, as well as its crossed counterpart, represents the effect of the medium, and vanishes as $n_0 \to 0$. The various terms in Eq. (3.25) can be classified in terms of the on- or off-shell pions or nucleons they contain in intermediate states. In the first term under the integral sign the intermediate pion is on shell, the nucleon in general being off shell. The opposite situation prevails in the second term under the integral sign, because then the nucleon is on shell.[33]

As before, we seek amplitudes $h_\alpha(\omega)$ of good isospin and spin such that

$$f(\vec{q}, \vec{q}'; \omega) = \sum_\alpha P_\alpha(\vec{q}', \vec{q}) h_\alpha(\omega) . \tag{3.26}$$

The h_α in this expression is an effective amplitude in the medium and of course differs from the $\overset{0}{h}_\alpha$ of Eq. (3.6). The projection technique that gave us Eq. (3.11) goes through as before for the first term in the curly brackets of Eq. (3.25) as well as its crossed counterpart. For the density-dependent terms, the factors $n(\vec{q}-\vec{p})$ and its crossing partner, $n(-\vec{q}'-\vec{p})$, place angular restrictions on the integral $d\Omega_{\vec{p}}$. As a consequence, one finds that Eq. (3.8) is replaced by the more general one

$$\int d\Omega_{\vec{p}}\, n(\vec{q}-\vec{p}) P_\alpha(\vec{q}', \vec{p}) P_\beta(\vec{p}, \vec{q}) = 4\pi p^2 P_\alpha(\vec{q}', \vec{q}) \Delta_{\alpha\beta} \tag{3.27}$$

that is nondiagonal in the total spin J. The $\Delta_{\alpha\beta}$ are the elements of the following 4×4 matrix:

$$(\Delta_{\alpha\beta}) = \begin{pmatrix} \Delta' & 0 \\ 0 & \Delta' \end{pmatrix}; \quad \Delta' = \begin{pmatrix} \bar{1} & 2\bar{P}_2 \\ \bar{P}_2 & \bar{1}+\bar{P}_2 \end{pmatrix}, \tag{3.28}$$

where $P_2 = \frac{1}{2}(3\cos\theta_{\vec{p}\vec{q}} - 1)$, and the bar indicates the restricted angular average $\int n(\vec{q}-\vec{p})d\Omega_{\vec{p}}/4\pi$. The $\Delta_{\alpha\beta}$ are independent of the isospin T. Thus amplitudes h_α of the same isospin, but different J, are coupled by $\Delta_{\alpha\beta}$. The equations for the new h_α's are

$$h_\alpha(\omega) = \frac{\lambda_\alpha}{\omega} + \frac{1}{\pi}\int_\mu^\infty d\omega_{\vec{p}}\, p^3 v^2(p)\left(\frac{|h_\alpha(\omega_{\vec{p}})|^2}{\omega_{\vec{p}} - \omega - i\delta} + \sum_\beta A_{\alpha\beta}\frac{|h_\beta(\omega_{\vec{p}})|^2}{\omega_{\vec{p}} + \omega - i\delta}\right) - 4\pi\left[M_\alpha(\omega) + \sum_\beta A_{\alpha\beta}M_\beta(-\omega)\right], \tag{3.29}$$

where $\lambda_\alpha \neq \overset{0}{\lambda}_\alpha$ is the renormalized coupling constant in the medium. The functions M_α are defined by $M_\alpha(\omega) = \sum_\beta I_{\alpha\beta}h^*_\alpha(\omega)h_\beta(\omega)$, where

$$I_{\alpha\beta} = 4\pi\int_0^{p_F+q}\frac{dp}{(2\pi)^3}\frac{p^4\Delta_{\alpha\beta}}{(\omega_{\vec{p}} - i\delta)^2 - \omega^2}. \tag{3.30}$$

The integrals $I_{\alpha\beta}$ are complicated functions of the input energy ω and the pion momentum $\vec{q}$ in the medium. A useful simplification occurs if we replace $\vec{q}$ by the incident momentum $\vec{p}$. Then the functions $I_{\alpha\beta}$, and hence the amplitudes h_α, become functions of ω alone. The $\vec{q}$ dependence of the forward-scattering amplitudes $f(\vec{q}, \vec{q}; \omega) \sim q^2$ is then isolated in the projectors P_α in Eq. (3.26). Consequently we will always have $\Pi(q) \propto q^2$, leading via Eq. (2.11) to a simple equation for the refractive index $n(\omega)$. If we keep the full dependence on $\vec{q}$ in the $I_{\alpha\beta}$, the amplitudes h_α will depend on $\vec{q}$ as well as ω, and thus on $n(\omega)$. Equation (2.11) would then become a complicated implicit equation for $n(\omega)$. We argue that our approximation $\vec{q} \simeq \vec{p}$ in $I_{\alpha\beta}$ neglects terms of order $[n(\omega) - 1]$ and thus should be good at low densities. However, this point deserves further study.[34] Using this approximation, we find that

$$\begin{aligned}
M_{11}(\omega) &= I(\omega)|h_{11}(\omega)|^2 + 2[\tilde{I}(\omega) - I(\omega)]h^*_{11}(\omega)h_{13}(\omega),\\
M_{13}(\omega) &= \tilde{I}(\omega)|h_{13}(\omega)|^2 + [\tilde{I}(\omega) - I(\omega)]h^*_{13}(\omega)h_{11}(\omega),\\
M_{31}(\omega) &= I(\omega)|h_{31}(\omega)|^2 + 2[\tilde{I}(\omega) - I(\omega)]h^*_{31}(\omega)h_{33}(\omega),\\
M_{33}(\omega) &= \tilde{I}(\omega)|h_{33}(\omega)|^2 + [\tilde{I}(\omega) - I(\omega)]h^*_{33}(\omega)h_{31}(\omega).
\end{aligned} \tag{3.31}$$

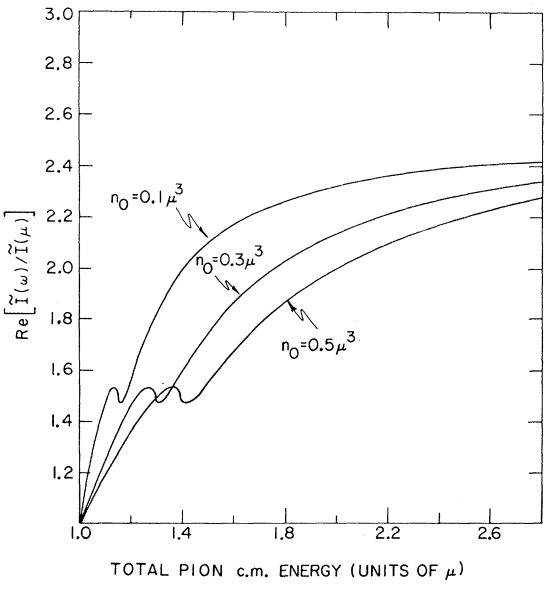

FIG. 9. The real part of the ratio $\tilde{I}(\omega)/\tilde{I}(\mu)$ as a function of ω for values of density $n_0 = 0.1$, 0.3, $0.5\mu^3$ of interest for the nuclear problem.

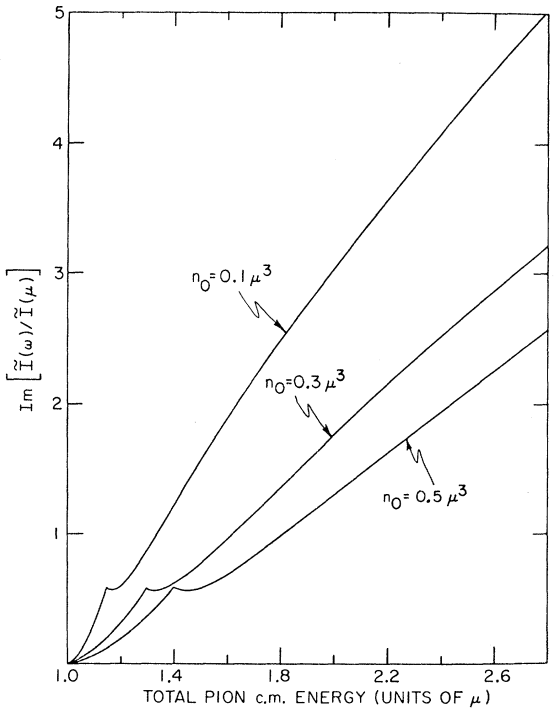

FIG. 10. The imaginary part of the ratio $\tilde{I}(\omega)/\tilde{I}(\mu)$ as a function of total pion c.m. energy ω for densities $n_0 = 0.1$, 0.3, $0.5\mu^3$.

In terms of the dimensionless variable $\beta = p/p_F$ the functions $I \equiv I_{11,11}$ and $\tilde{I} \equiv I_{13,13}$ are given by

$$\begin{aligned}
\mathrm{Re}I(\omega) &= \frac{n_0}{4}\left[1+\frac{3}{2}\beta^2-\frac{3}{8}\beta(1-4\beta^2)\ln\left|\frac{1-2\beta}{1+2\beta}\right|\right],\\
\mathrm{Im}I(\omega) &= \frac{n_0}{4}\begin{cases}\frac{3\pi}{2}\beta^3, & \beta<\frac{1}{2}\\ \frac{3\pi}{8}\beta, & \beta>\frac{1}{2}\end{cases},\\
\mathrm{Re}\tilde{I}(\omega) &= \frac{n_0}{4}\left[\frac{15}{8}+\frac{3}{2}\beta^2-\frac{3}{16\beta^2}+\frac{1}{2}\left(3\beta^3-\frac{3}{2}\beta+\frac{9}{16\beta}-\frac{3}{32\beta^3}\right)\ln\left|\frac{1-2\beta}{1+2\beta}\right|\right],\\
\mathrm{Im}\tilde{I}(\omega) &= \frac{n_0}{4}\begin{cases}\frac{3\pi}{2}\beta^3, & \beta<\frac{1}{2}\\ \frac{3\pi}{4}\left(\beta-\frac{3}{8\beta}+\frac{1}{16\beta^3}\right), & \beta>\frac{1}{2}\end{cases}.
\end{aligned} \tag{3.32}$$

Equation (3.29) is the main result of this section. It constitutes a set of coupled, nonlinear integral equations for the functions $h_\alpha(\omega)$ that determine the scattering amplitude of a pion from a nucleon in a nuclear medium. In the zero-density limit $n_0 \to 0$ both functions I and $\tilde{I}$ vanish and we regain the Chew-Low equation (3.11).

Let us note some features of the functions I and $\tilde{I}$. For small p (i.e $\omega \sim \mu$) I and $\tilde{I}$ are real functions

$$\begin{aligned}
I(\omega) &\simeq \frac{n_0}{4}(1+3\beta^2+\cdots),\\
I(\omega) &\simeq \frac{n_0}{4}\left(1+\frac{18}{5}\beta^2+\cdots\right).
\end{aligned} \tag{3.33}$$

For large $p(p \gg p_F)$ we have

$$\begin{aligned}
\mathrm{Re}I(\omega) &\simeq \frac{n_0}{4}\left(\frac{5}{4}+\frac{1}{90\beta^2}+\cdots\right),\\
\mathrm{Re}\tilde{I}(\omega) &\simeq \frac{n_0}{4}\left(\frac{5}{2}-\frac{17}{40\beta^2}+\cdots\right).
\end{aligned} \tag{3.34}$$

The behavior of $\tilde{I}$ as a function of ω is illustrated in Figs. 9 and 10 for various values of the density n_0. The curves for I are very similar and are not reproduced here. The curious loops in $\mathrm{Re}\tilde{I}$ and the kinks in $\mathrm{Im}\tilde{I}$ are caused by the logarithmic singularity in the first derivative at $p = \frac{1}{2}p_F$.

C. Properties of the Effective Amplitude $h_\alpha(\omega)$ in Nuclear Matter

Let us compare some properties of the solutions $h_\alpha(\omega)$ of Eq. (3.29) with their free pion-nucleon counterparts that are solutions of the Chew-Low equation (3.11). We easily deduce the following properties of $\overset{0}{h}$ and h:

(i) Crossing symmetry: Both $\overset{0}{h}$ and h satisfy the Chew-Low crossing relation[27]

$$h_\alpha(\omega) = \sum_\beta A_{\alpha\beta} h_\beta(-\omega). \tag{3.35}$$

(ii) Unitarity: Taking the imaginary part of Eq. (3.11) one sees that

$$\begin{aligned}
&\mathrm{Im}\overset{0}{h}_\alpha(\omega) = \frac{1}{2i}[\overset{0}{h}_\alpha(\omega+i\delta)-\overset{0}{h}_\alpha(\omega-i\delta)] = p^3|\overset{0}{h}_\alpha(\omega)|^2,\\
&\omega = (p^2+\mu^2)^{1/2},
\end{aligned} \tag{3.36}$$

which is the condition that $\overset{0}{h}_\alpha$ is unitary. Equation (3.36) ensures that the physical amplitude $\overset{0}{h}_\alpha(\omega)$ has a representation

$$\overset{0}{h}_\alpha(\omega) = \frac{1}{p^3(\cot\overset{0}{\delta}_\alpha - i)} \tag{3.37}$$

in terms of a real phase shift $\overset{0}{\delta}_\alpha$.

The corresponding relation for $h_\alpha(\omega)$ is only simple if we neglect the crossing term $\sum_\beta A_{\alpha\beta} M_\beta(-\omega)$ in Eq. (3.29). Then

$$\mathrm{Im}h_\alpha(\omega) = p^3|h_\alpha(\omega)|^2 - 4\pi\,\mathrm{Im}M_\alpha(\omega). \tag{3.38}$$

However for $p < \frac{1}{2}p_F$,

$$4\pi\,\mathrm{Im}M_\alpha(\omega) = p^3|h_\alpha(\omega)|^2 + 4\pi\sum_\beta \mathrm{Re}I_{\alpha\beta}\,\mathrm{Im}(h_\alpha^* h_\beta), \tag{3.39}$$

since $4\pi\,\mathrm{Im}I_{\alpha\beta} = p^3\delta_{\alpha\beta}$ in this case. Therefore, the right-hand side of Eq. (3.38) vanishes for $p < \frac{1}{2}p_F$:

$$\mathrm{Im}h_\alpha(\omega) = 0, \quad p < \tfrac{1}{2}p_F. \tag{3.40}$$

This is so because the first term in Eq. (3.39) cancels a similar one in Eq. (3.38). We are thus left with a homogeneous set of equations in $\mathrm{Im}h_\alpha$ that can only have the trivial solution (3.40). The result (3.40) has the rather remarkable implication that the presence of the nuclear medium changes

the threshold energy from μ to

$$\tilde{\mu} = \left[\mu^2 + \left(\frac{p_F}{2}\right)^2\right]^{1/2} \tag{3.41}$$

which is density-dependent. The physical reason for $\mathrm{Im}h_\alpha$ vanishing at $\omega = \tilde{\mu}$ is related to the Pauli principle. Looking at Fig. 6 for example, we recall that the intermediate pion-nucleon state is real only if both particles are on shell and share the input energy, $\omega = \omega_{\vec{q}} = \omega_{\vec{q}-\vec{p}}$. In the static limit, the energy conserving condition is equivalent to[35]

$$|\vec{q}| = |\vec{q} - \vec{p}|, \quad \text{or} \quad \cos\theta_{\vec{p}\vec{q}} = \frac{p}{2q}. \tag{3.42}$$

For an isolated nucleon ($p_F = 0$) one can satisfy Eq. (3.42) for any $\vec{p}$, so that there is no lower bound on $\vec{q}$. However, if the nucleon $\vec{p}$ forms part of a Fermi sea, then we can only promote particles to states outside the Fermi sphere $|\vec{p}| > p_F$. The smallest value of $|\vec{q}|$ that still allows this to happen is $|\vec{q}| = \frac{1}{2}p_F$ according to Eq. (3.42), leading to the threshold $\omega = \tilde{\mu}$. Numerically the change is not small. For a representative value $p_F \simeq 2\mu$ in nuclear matter, one has $\tilde{\mu} - \mu = (\sqrt{2} - 1)\mu \simeq 60$ MeV.

The condition (3.40) is exact if crossing is neglected. For $\omega > \tilde{\mu}$ the relation between $\mathrm{Im}h_\alpha$ and $|h_\alpha|^2$ is complicated by the coupling terms in M_α. To the extent that this channel-channel coupling can be ignored, one has

$$\begin{aligned}\mathrm{Im}h_\alpha(\omega) &= \frac{1}{2i}[h_\alpha(\omega + i\delta) - h_\alpha(\omega - i\delta)] \\ &= (p^3 - 4\pi\,\mathrm{Im}I_{\alpha\alpha})|h_\alpha(\omega)|^2\end{aligned} \tag{3.43}$$

a result which means that

$$h_\alpha(\omega) = \frac{1}{(p^3 - 4\pi\,\mathrm{Im}I_{\alpha\alpha})(\cot\delta_\alpha - i)}, \tag{3.44}$$

where $\delta_\alpha \neq \overset{0}{\delta}_\alpha$ is real. The only zero of $(p^3 - 4\pi\,\mathrm{Im}I_{\alpha\alpha})$ is at $p = \frac{1}{2}p_F$. The condition (3.43) plus the fact that $h_\alpha(\omega)$ is finite at $\omega = \tilde{\mu}$ implies that the phase shifts δ_α must go to zero like $\delta_\alpha \propto p_F{}^2(p - \frac{1}{2}p_F)$ at $p = \frac{1}{2}p_F$ in contrast to the $\overset{0}{\delta}_\alpha$ that behave like p^3 near $p = 0$.

D. Low-Energy Pion Optical Potential—Quenching

A useful expression for the pion optical potential can be derived in the limit of low energy and density, where the $h_\alpha(\omega)$ approach values independent of ω. This amounts to making the effective-range approximation in Eq. (3.29). We thus calculate $h_\alpha(\omega)$ under the following two approximations: (i) evaluate the $I_{\alpha\beta}$ at threshold $\omega = \mu$ and, (ii) replace the $h_\alpha(\omega)$ on the right-hand side of Eq. (3.29) by the zero-density solutions $\overset{0}{h}_\alpha(\omega)$ of Eq. (3.11).

Thus $I_{\alpha\beta} \simeq N_0\delta_{\alpha\beta}$ and

$$\begin{aligned}h_\alpha(\omega) \simeq \overset{0}{h}_\alpha(\omega) - 4\pi N_0[\,|\overset{0}{h}_\alpha(\omega)|^2 \\ + \sum_\beta A_{\alpha\beta}|\overset{0}{h}_\beta(-\omega)|^2\,],\end{aligned} \tag{3.45}$$

where $N_0 = \frac{1}{4}n_0$ is the density of nucleons of given spin and charge.

We next show that the approximate expression (3.45) leads directly[36] to the p-wave optical potential derived previously from multiple-scattering theory.[26,37] To do so, we must first generalize Eq. (3.23) to include scattering from more than one type of scatterer (protons and neutrons). Noting that only coherent forward scattering of pions enters the picture, we see that the amplitude $f(\vec{q}, \vec{q})$ in Eq. (3.23) is replaced by the average amplitude

$$f_{\mathrm{coh}} = \tfrac{1}{4}\sum_{\sigma\tau}\langle\pi^-\sigma\tau|f(\vec{q},\vec{q})|\pi^-\sigma\tau\rangle = \tfrac{1}{3}q^2\sum_\alpha v_\alpha h_\alpha(\omega), \tag{3.46}$$

where $v_\alpha = (1, 2, 2, 4)$ for π^- scattering. The latter form of f_{coh} follows upon introducing the expansion (3.26) for f in the forward direction. The result (3.46) is still independent of any approximations one might use for h_α. The low-energy approximation (3.45) gives

$$f_{\mathrm{coh}} \simeq \tfrac{1}{3}q^2[\sum_\alpha v_\alpha\overset{0}{h}_\alpha(\omega) - 8\pi N_0\sum_\alpha v_\alpha|\overset{0}{h}_\alpha(\omega)|^2], \tag{3.47}$$

the direct and crossing terms contributing *equally*. This comes about as follows. The identities

$$\sum_\alpha v_\alpha A_{\alpha\beta} = v_\beta, \quad \sum_\beta v_\beta A_{\beta\gamma}A_{\beta\delta} = v_\gamma\delta_{\gamma\delta} \tag{3.48}$$

plus the crossing relation (3.35) show that

$$\begin{aligned}\sum_{\alpha\beta} v_\alpha A_{\alpha\beta}|\overset{0}{h}_\beta(-\omega)|^2 &= \sum_\beta v_\beta|\overset{0}{h}_\beta(-\omega)|^2 \\ &= \sum_\gamma v_\gamma|\overset{0}{h}_\gamma(\omega)|^2\end{aligned} \tag{3.49}$$

and Eq. (3.47) follows directly. Replacing the $\overset{0}{h}_\alpha$ at low energies by the appropriate scattering volumes C_α, one obtains

$$f_{\mathrm{coh}} \simeq q^2\left[\frac{1}{3}\sum_\alpha v_\alpha C_\alpha - \frac{8\pi N_0}{3}\sum_\alpha v_\alpha C_\alpha{}^2\right] \tag{3.50}$$

for the low-energy coherent scattering amplitude. Notice that the free-space amplitude is always *quenched* by the presence of the medium, in agreement with the results of Refs. 26 and 37. To make contact with previous work,[26,37] we introduce the

linear combinations C_{2T} and $\tilde{C}_{2T}$,

$$C_1 = C_{11} + 2C_{13}, \quad \tilde{C}_1 = (C_{11} - C_{13}),$$
$$C_3 = C_{31} + 2C_{33}, \quad \tilde{C}_3 = (C_{31} - C_{33}), \tag{3.51}$$

that are indexed by the channel isospin $2T$. The p-wave part of the πN scattering amplitude then becomes

$$f(\vec{q}, \vec{q}') = (C_1 P_{1/2} + C_3 P_{3/2})(\vec{q} \cdot \vec{q}') + i(\tilde{C}_1 P_{1/2} + \tilde{C}_3 P_{3/2})[\vec{\sigma} \cdot (\vec{q} \times \vec{q}')], \tag{3.52}$$

where $P_{1/2}$ and $P_{3/2}$ are isospin projection operators. Nonzero values of the $\tilde{C}$ measure the importance of the spin dependence of the scattering amplitude f. The sums of scattering volumes entering Eq. (3.50) are given by

$$\tfrac{1}{3}\sum_\alpha v_\alpha C_\alpha = \tfrac{1}{3}(C_1 + 2C_3);$$
$$\sum_\alpha v_\alpha C_\alpha^2 = \tfrac{1}{3}(C_1^2 + C_3^2) + \tfrac{2}{3}(\tilde{C}_1^2 + \tilde{C}_3^2). \tag{3.53}$$

Values of the constants C_{2T} and $\tilde{C}_{2T}$ can be calculated from the tabulation in Ref. 38. We have

$$C_1 = -0.28, \quad \tilde{C}_1 = +0.11,$$
$$C_3 = +0.27, \quad \tilde{C}_3 = -0.33 \tag{3.54}$$

in units of $1/\mu^3$, so that the spin-flip contribution ($=0.47\mu^{-6}$) to $\sum_\alpha v_\alpha C_\alpha^2$ is about twice the non-spin-flip contribution ($=0.22\mu^{-6}$). On the other hand, if one simply neglects spin-flip terms, the sums in Eq. (3.53) can be reexpressed in the form

$$\tfrac{1}{3}\sum_\alpha v_\alpha C_\alpha = \frac{C_n + C_p}{2};$$
$$\sum_\alpha v_\alpha C_\alpha^2 = \frac{C_n^2 + C_p^2}{2} + \frac{(C_n - C_p)^2}{4}, \tag{3.55}$$

where $3C_p = 2C_1 + C_3$, $C_n = C_3$.

The pion self-energy can now be computed from Eqs. (3.50) and (3.23). The result is

$$\Pi(\vec{q}, \omega) \simeq 4\pi n_0 q^2 \left[\frac{1}{3}\sum_\alpha v_\alpha C_\alpha - \frac{4\pi n_0}{3}\left(\frac{1}{4}\sum_\alpha v_\alpha C_\alpha^2\right)\right], \tag{3.56}$$

where either of Eqs. (3.53) or (3.55) determine the quantities in round parentheses. Numerically the set (3.53) is to be preferred. The opposite approximation (3.55) of assuming spin-independent amplitudes leads to the result[37]

$$\Pi(\vec{q}, \omega) = 4\pi n_0 q^2 \left[\frac{C_n + C_p}{2} - \frac{4\pi n_0}{3} \times \frac{1}{4}\left(\frac{C_n^2 + C_p^2}{2} + \frac{(C_n - C_p)^2}{4}\right)\right] \tag{3.57}$$

that was also derived in Ref. 26 using a different technique.[39] We have thus established the connection between the present approach and the density expansion method of Ref. 26, which is appropriate to the problem of pionic atoms, i.e. pion-nucleus scattering near threshold.

E. Pion Optical Potential near the (3,3) Resonance

The low-energy expansion (3.50) and the resulting pion-nucleus potential are expected to break down in the vicinity of the πN resonance in the (3, 3) channel. The low-energy small parameter $n_0 C_0 \approx 0.05$, where C_0 is the average scattering volume $\frac{1}{2}(C_n + C_p)$ gets replaced by $\lambda\!\!\!^{-}/r_0$, where $\lambda\!\!\!^{-}$ is the pion wavelength at resonance, and r_0 the internucleon spacing, see Sec. III F. We are therefore faced with a different meaning of low density. On the other hand, the (3, 3) channel certainly dominates in the resonance region. Therefore we write

$$f_{\rm coh} \approx \frac{4}{3} q^2 h(\omega), \tag{3.58}$$

where $h \equiv h_{33}$ is the amplitude in this channel. The neglect of all other channels means that h satisfies the following truncated version of Eq. (3.29)[40]

$$h(\omega) = \frac{\lambda}{\omega} + \frac{1}{\pi}\int_\mu^\infty d\omega_{\vec{p}}\, p^3 v^2(p) \times \frac{|h(\omega_{\vec{p}})|^2}{\omega_{\vec{p}} - \omega - i\delta} - 4\pi \tilde{I}(\omega)|h(\omega)|^2 \tag{3.59}$$

The quantity $\tilde{I}$ has been introduced in Eqs. (3.31) and (3.32), and the coupling parameter $\lambda = \frac{4}{3} f_r^2 / 4\pi\mu^2$ is the renormalized pion-nucleon coupling strength, *including* renormalization effects of the medium. An analytical solution of Eq. (3.59) has so far eluded us, although its zero-density version with $\tilde{I} = 0$ is simple to solve.[27] In this section we therefore neglect the density dependence in h and set $h = \overset{0}{h}$, where $\overset{0}{h}$ is the known solution of the Chew-Low equation at zero density. This will give us an expression for $f_{\rm coh}$ that is valid at resonance, provided only that the density is low enough, i.e. $\lambda\!\!\!^{-} \ll r_0$. The results obtained in such an approximation lead to a description of pion-nucleus resonant scattering that resembles the model proposed by Ericson and Hüfner.[20] We improve on this approximation in the next section.

The Chew-Low (3, 3) resonance amplitude is obtained by solving Eq. (3.59) in closed form at zero density. The result is a function of the form[27]

$$\frac{\overset{0}{\lambda}}{\omega}\overset{0}{h}{}^{-1}(\omega) = 1 - \frac{\omega}{\pi}\int_\mu^\infty \frac{d\omega_{\vec{p}}}{\omega_{\vec{p}}^2} p^3 v^2(p) \frac{\overset{0}{\lambda}}{\omega_{\vec{p}} - \omega - i\delta} = \left[1 - \frac{\omega}{\omega_0} - \frac{i\Gamma(\omega)}{2\omega_0}\right] \tag{3.60}$$

if one neglects Castillejo, Dalitz, and Dyson (CDD) poles.[41] From Eq. (3.60), we see that $\overset{0}{h}(\omega)$ displays a resonance having an energy-dependent width

$$\Gamma(\omega) = 2\overset{0}{\lambda} p^3 v^2(p) \frac{\omega_0}{\omega} \tag{3.61}$$

and a resonance energy ω_0 that is also a function of ω:

$$\omega_0^{-1} \equiv \omega_0(\omega)^{-1} = \frac{P}{\pi} \int_\mu^\infty \frac{d\omega_{\vec{p}}}{\omega_{\vec{p}}^2} \frac{\overset{0}{\lambda} p^3 v^2(p)}{\omega_{\vec{p}} - \omega} , \tag{3.62}$$

where P indicates the principal value. The result (3.60) gives the effective range expansion of $\mathrm{Re}\overset{0}{h}^{-1}(\omega)$ if ω_0 is replaced by a constant.

We can now calculate the pion self-energy as before. However, at incident pion kinetic energies ~200 MeV, one can estimate scattering cross sections semiclassically without passing to phase shifts first via an optical potential. To this end, we require the nuclear refractive index $n(\omega)$ given by Eq. (2.11). One finds from Eqs. (3.46) and (2.11) that

$$n^2(\omega) - 1 = \left[\frac{4\pi}{3} \sum_\alpha v_\alpha \int_0^{n_0} dn_0' \, h_\alpha(\omega) \right] n^2(\omega) \tag{3.63}$$

without approximation. The appearance of $n^2 = q^2/p^2$ on the right-hand side of Eq. (3.63) is a specific feature of the p-wave nature of the interaction. We solve for n^2 after introducing the abbreviation

$$\alpha(\omega) = \frac{4\pi}{3} \sum_\alpha v_\alpha \int_0^{n_0} dn_0' \, h_\alpha(\omega, n_0') \tag{3.64}$$

to find[42]

$$n^2(\omega) - 1 = \frac{\alpha(\omega)}{1 - \alpha(\omega)} . \tag{3.65}$$

The resonance approximation (3.58) only considers the (3, 3) channel in computing $\alpha(\omega)$. There is, however, a technical difficulty in this procedure. In principle, the expression (3.60) gives the πN scattering amplitude in the center-of-mass system, although this fact is not obvious in the Chew-Low equations because the static limit has been taken.[43] On the other hand, the h's appearing in Eq. (3.64) refer to the laboratory system. We effect the transformation from the lab amplitude $h_\alpha(\omega_p)$ to the center-of-mass amplitude $h_\alpha(\omega_\kappa)$ by using the relation $p\, h_\alpha(\omega_p) = \kappa h_\alpha(\omega_\kappa)$, where κ and $\omega_\kappa = (\kappa^2 + \mu^2)^{1/2}$ are the pion center-of-mass momentum and energy, and p and $\omega_p = (p^2 + \mu^2)^{1/2}$ are the corresponding lab quantities.[44] One can then calculate α in terms of the amplitudes $h_\alpha(\omega_\kappa)$ in the center-of-mass system. Taking the (3, 3) channel only and setting $\eta = \kappa/p$ one has

$$\alpha(\omega) \simeq \frac{16\pi}{3} n_0 \eta \overset{0}{h}(\omega_\kappa) \tag{3.65'}$$

at low densities. The function $\overset{0}{h}(\omega_\kappa)$ is given by Eq. (3.60) with $\omega \to \omega_\kappa$ and $p \to \kappa$. Using the estimate (3.65') for α, one has

$$n_{\mathrm{CL}}^2(\omega) - 1 = \frac{\Delta(\omega_\kappa)}{\omega_0(\omega_\kappa) - \omega_\kappa - \Delta(\omega_\kappa) - i[\Gamma(\omega_\kappa)/2]} , \tag{3.66}$$

i.e., a resonant form that exhibits a *shifted* resonance energy, with shift function $\Delta(\omega_\kappa)$ given by

$$\Delta(\omega_\kappa) = \frac{8\pi n_0 \Gamma(\omega_\kappa)}{3\kappa^3} . \tag{3.67}$$

We append the subscript CL to n to emphasize the origin of the approximation (3.66). This expression has some features in common with the Ericson-Hüfner model.[20] In Sec. IV we compare the results based on an exact calculation of $n(\omega)$ with the first-order approximation $n_{\mathrm{CL}}(\omega)$.

We close this section with some qualitative remarks concerning the use of the simple propagators G of Eq. (3.19) and D_0 of Eq. (2.5) to describe nucleon and pion propagation in intermediate states. As pointed out previously, our method specifically excludes the renormalization of pion lines in intermediate states. However, there are some indications in the literature[45] that the pion-propagator renormalization is not important.

The renormalization of nucleon lines is allowed in our approach, as per Eq. (3.18). A complete calculation of these effects requires a knowledge of the nucleon self-energy $\Sigma(p)$. The contributions to $\Sigma(p)$ can be roughly classified as (i) average field effects, in which the medium remains unexcited, and (ii) polarization of the medium by the probe nucleon. Our model does not include polarization effects. However, to the extent that the average field effects (binding-energy corrections) can be described by assigning to the nucleon an effective mass m^*, we have

$$\epsilon_{\vec{p}}^{\,*} = \frac{p^2}{2m} + \Sigma(\vec{p}) \simeq \frac{p^2}{2m^*} + \Sigma_0 , \tag{3.68}$$

where Σ_0 is a constant. One then finds that

$$\int \frac{dp_0}{2\pi} D_0(p) G(k + q - p) \simeq \frac{i}{2\omega_{\vec{p}}} \frac{1}{\epsilon_{\vec{k}+\vec{q}-\vec{p}}^{\,*} - \epsilon_{\vec{k}}^{\,*} - q_0 + \omega_{\vec{p}} - i\delta} \tag{3.69}$$

replaces the cofactor of $f^\dagger f$ in Eq. (3.4). Since only *differences* of single-particle energies enter this expression, the constant Σ_0 cancels out. If we now pass to the static limit, Eq. (3.69) leads

to the same result as that given by Eq. (3.4) without nucleon line renormalizations. One expects such a result to hold, whether or not the effective mass description is valid, as long as nucleon self-energies are small relative to the pion mass μ. One knows empirically that $|\Sigma| \sim 50$ MeV for nucleons deep in the Fermi sea, with Σ decreasing slowly with increasing momentum. Consequently, the condition $|\Sigma| \ll \mu$ seems reasonably well satisfied and we conclude that the Pauli principle modifications in $G(p)$ are the important ones. A *quantitative* assessment of this opinion must of course await a proper calculation of Σ both on and off the nucleon energy shell.

F. Iterative Solution for the Pion Optical Potential near Resonance

We finally address ourselves to the question of obtaining a solution for $\Pi(q)$ under a minimum number of approximations. We have devised the following iterative scheme that is carried through numerically in the next section. We retain the two assumptions of Sec. III E, i.e., that only the (3, 3) channel is important and that crossing terms can be neglected. Then the discussion leading to Eq. (3.44) is valid. For the (3, 3) channel in particular, one has ($\delta \equiv \delta_{33}$)

$$h_{33}(\omega) \equiv h(\omega) = \frac{1}{(p^3 - 4\pi \operatorname{Im}\tilde{I})(\cot\delta - i)}, \quad \omega > \tilde{\mu}. \tag{3.70}$$

We now return to Eq. (3.59) and cast it into a form that contains $\cot\delta$ as the unknown function, since the structure (3.70) automatically satisfies the unitarity requirement on h. Define the auxiliary function

$$F(\omega) = h(\omega) + 4\pi \tilde{I}(\omega)|h(\omega)|^2. \tag{3.71}$$

Then

$$F(\omega) = \frac{\lambda}{\omega} + \frac{1}{\pi}\int_\mu^\infty d\omega_{\vec{p}}\, p^3 v^2(p) \frac{|h(\omega_{\vec{p}})|^2}{\omega_{\vec{p}} - \omega - i\delta} \tag{3.72}$$

has exactly the *same* singularities (a pole at $\omega = 0$ and a cut from μ to ∞ along the real ω axis) as the Chew-Low function $\overset{0}{h}(\omega)$ of Eq. (3.60), which is a solution of Eq. (3.59) with $n_0 = 0$. Thus a representation for $F(\omega)$ can be found by following the same procedure[27] as Chew and Low use for constructing $\overset{0}{h}(\omega)$. Introduce the inverse of $F(\omega)$ via

$$g(\omega) = \frac{\lambda}{\omega}\frac{1}{F(\omega)} \tag{3.73}$$

to remove the pole at $\omega = 0$. Then $g(\omega)$ only has a cut from μ to ∞, and approaches a constant as $\omega \to -\infty$. Thus $g(z)$ has a representation [the value $g(0) = 1$ is fixed by the choice (3.73)] of the form

$$g(z) = 1 - \frac{\lambda z}{\pi}\int_\mu^\infty \frac{d\omega_{\vec{p}}}{\omega_{\vec{p}}^2}\, p^3 v^2(p) \frac{\rho(\omega_{\vec{p}})}{\omega_{\vec{p}} - z} \tag{3.74}$$

as a function of the complex variable z, where $g(\omega)$ now has the meaning

$$\lim_{\delta \to 0^+} g(z), \quad z = \omega + i\delta.$$

The spectral function $\rho(\omega)$ is determined by the "jump" of $g(z)$ across the cut starting at $\omega = \tilde{\mu}$:

$$\frac{1}{2i}[g(\omega + i\delta) - g(\omega - i\delta)] = \frac{-1}{\omega}\frac{\lambda p^3}{|1 + 4\pi\tilde{I}(\omega)h^*(\omega)|^2} = \frac{-\lambda p^3}{\omega\rho(\omega)}$$

or

$$\rho(\omega) = \frac{1}{|1 + 4\pi\tilde{I}(\omega)h^*(\omega)|^2}. \tag{3.75}$$

Equation (3.74) can now be rewritten as an equation for $h(\omega)$ containing the *modified coupling parameter* λ':

$$\lambda'(\omega) = \lambda\rho(\omega) = \frac{\lambda}{|1 + 4\pi\tilde{I}(\omega)h^*(\omega)|^2}. \tag{3.76}$$

We find the following equation for $h(\omega)$:

$$\frac{\lambda'(\omega)}{\omega}[h^{-1}(\omega) + 4\pi\tilde{I}^*(\omega)] = 1 - \frac{\omega}{\pi}\int_\mu^\infty \frac{d\omega_{\vec{p}}}{\omega_{\vec{p}}^2}\, p^3 v^2(p) \frac{\lambda'(\omega_{\vec{p}})}{\omega_{\vec{p}} - \omega - i\delta}. \tag{3.77}$$

This result can be cast into the form of an effective-range expansion for $h^{-1}(\omega)$,

$$\frac{\lambda'}{\omega}h^{-1}(\omega) = \left[1 - \frac{4\pi\lambda' J}{\omega} - \frac{\omega}{\omega_0'} - \frac{i}{2}\frac{\tilde{\Gamma}(\omega)}{\omega_0'}\right] \tag{3.78}$$

in terms of (energy-dependent) parameters

$$(\omega_0')^{-1} = \frac{P}{\pi}\int_\mu^\infty \frac{d\omega_{\vec{p}}}{\omega_{\vec{p}}^2}\, p^3 v^2(p) \frac{\lambda'(\omega_{\vec{p}})}{\omega_{\vec{p}} - \omega} \tag{3.79}$$

and

$$\tilde{\Gamma}(\omega) = 2\lambda' p^3 v^2(p)\frac{\omega_0'}{\omega}\left(1 - \frac{4\pi K}{p^3}\right), \tag{3.80}$$

after writing $\tilde{I}(\omega) = J + iK$. If ω_0' and $\tilde{\Gamma}$ are slowly varying functions of ω, Eq. (3.78) shows that $h(\omega)$ resonates near $\omega = \tilde{\omega}_0$, where

$$\tilde{\omega}_0 = \omega_0'\left[1 - \frac{4\pi\lambda' J}{\omega}\right]. \tag{3.81}$$

Since the amplitude given by (3.78) is automatically unitary in the sense of Eq. (3.43), we concentrate on the real part only. For $\omega < \tilde{\mu}$ the function $h(\omega)$ is purely real and given by Eq. (3.78)

with $\tilde{\Gamma} \equiv 0$. For $\omega > \tilde{\mu}$ we write $\mathrm{Re}(h^{-1})$ in terms of $\cot\delta$, using Eq. (3.70). The equation for $\cot\delta$ then follows from Eq. (3.78):

$$\cot\delta = \frac{2}{\tilde{\Gamma}}(\tilde{\omega}_0 - \omega) . \tag{3.82}$$

Clearly, Eqs. (3.76) and (3.77) present us with the problem of determining $\lambda'(\omega)$ and $h(\omega)$ self-consistently, and we carry out such a program numerically in Sec. IV. However, the qualitative features of such a solution can be inferred from the key Eq. (3.76) for λ'. Near a resonance in $h(\omega)$, $[\mathrm{Re}h(\omega) = 0,\ \mathrm{Im}h(\omega) = (p^3 - 4\pi K)^{-1}]$ the factor $\rho(\omega)$ becomes

$$\rho_{\mathrm{res}} = \frac{(1 - 4\pi K/p^3)^2}{1 + (4\pi J/p^3)^2} < 1 \tag{3.83}$$

so that λ' is *always reduced* relative to λ, i.e. $\lambda' < \lambda$. Therefore, one expects that ω_0' shifts up relative to ω_0 (by about a factor $\rho_{\mathrm{res}}{}^{-1}$). The resonance energy $\tilde{\omega}_0$ in turn lies lower than ω_0' by the reduction factor shown in Eq. (3.81), so that the position of $\tilde{\omega}_0$ relative to the free πN resonance energy ω_0 is determined by which of these effects dominate.

At low energies, $\omega \simeq \mu$, the situation is different. Here $\mathrm{Im}h \approx 0$, while $\mathrm{Re}h \approx C$, where C is the scattering volume. Hence

$$\lambda' = \frac{\lambda}{(1 + 4\pi N_0 C)^2} , \quad \omega \cong \mu \tag{3.84}$$

and hence λ' is enhanced or reduced depending on the sign of C. The modification given by Eq. (3.84), which holds in every channel α, provided we neglect crossing terms, is closely related to the result (3.45). If we solve Eq. (3.29) in Born approximation with λ_α replaced by λ'_α, and identify the free πN scattering volumes C_α with λ_α/μ, then

$$h_\alpha(\mu) \simeq \frac{C_\alpha}{(1 + 4\pi N_0 C_\alpha)^2} . \tag{3.85}$$

Thus C_α is reduced or enhanced depending on its own sign. It is also interesting to compute $\Pi(q)$ from the above expression for $h(\mu)$. The result

$$\Pi(q) = \frac{4\pi n_0}{3} q^2 \sum_\alpha \frac{v_\alpha C_\alpha}{1 + 4\pi N_0 C_\alpha} , \quad \omega \sim \mu \tag{3.86}$$

is a Lorentz-Lorenz form for $\Pi(q)$ that reduces exactly to the Ericson-Ericson result,[37]

$$\Pi(q) = 4\pi q^2 \frac{N_0 C_0}{1 + 4\pi N_0 C_0/3} , \quad \omega \sim \mu$$

for low-energy pion scattering from one type of scatterer only, of density N_0. The scattering volume $C_0 = 3C$ in this case since the C_α assume a common value C. Notice that the expansion of Eq. (3.86) to order $n_0{}^2$ coincides with the earlier result (3.56), a property not shared by the Ericson-Ericson expression.[26,37]

The resonance and off-resonance values of the function $\rho(\omega)$ of Eq. (3.75) also show that "low density" has a different meaning in the two cases. If we are off resonance, we see from Eq. (3.84) that low density implies $4\pi N_0 C \propto n_0 C$ is small, while low density in Eq. (3.83) means that $4\pi J/p^3$ and $4\pi K/p^3$ are small. The latter condition is met for pion wavelengths $\ll$ internucleon spacing, $\lambda\!\!\!^{-} \ll r_0$. For pions near the (3, 3) resonance ($\lambda\!\!\!^{-} \approx 0.6/\mu$) in nuclear matter ($n_0 \approx 0.5\mu^3$), one finds that $\lambda\!\!\!^{-} \approx 0.7 r_0$, so that the resonance problem cannot be handled by perturbation expansions in the density.

We also see from Eq. (3.80) that the (3, 3) resonance width in nuclear matter $\tilde{\Gamma}$ is smaller than the free πN width Γ of Eq. (3.61) by a factor $\rho\omega_0'/\omega(1 - 4\pi K/p^3)$ if we assume $\lambda = \overset{0}{\lambda}$, i.e. neglect renormalization effects. This reduction in width comes partially from the factor $\rho(\omega)$ and partially from the action of the Pauli principle, represented by the factor $(1 - 4\pi K/p^3)$, that restricts the phase space available to the struck nucleon. Figure 15 shows a numerical illustration of this effect. One thus concludes that the (3, 3) resonance has a longer lifetime in nuclear matter than free space. Note, however, that this conclusion is based on the assumption of static nucleons. An average of the resonance widths in πN collisions in the nucleus over the Fermi distribution would result in a superposition of resonances, and hence a larger width. It is this Fermi-averaged resonance that is seen experimentally. We emphasize, however, that for a fixed nucleon momentum, the effect of the Pauli principle is to quench the (3, 3) resonance width.

G. Pion Optical Potential at Low Density—Quasiparticles

If the criterion of low density mentioned in the previous section is met at all energies, one can derive a pseudopotential for describing pion scattering by treating the pion as a quasiparticle[24] propagating according to the dispersion law (2.9):

$$\omega^2 = \mu^2 + q^2 - \Pi(\vec{q}, \omega) . \tag{2.9}$$

We look for quasiparticle excitations of the form $\omega = \omega_{\vec{q}} - i\gamma_{\vec{q}}$ that propagate with wave number $\vec{q}$:

$$(\omega_q - i\gamma_q)^2 = \mu^2 + q^2 - \Pi(\vec{q}, \omega_q - i\gamma_q) . \tag{3.87}$$

The quasiparticle solution of this equation assumes that the width $\gamma_{\vec{q}}$ is small, or that the lifetime τ of the quasiparticle is long, $\omega_{\vec{q}}\tau \gg 1$. Then

one can solve Eq. (3.87) as follows:

$$\omega_{\vec{q}}^2 \simeq \mu^2 + q^2 - \Pi_0(\vec{q}, \omega_{\vec{q}}),$$
$$\frac{1}{\tau} = 2\gamma_{\vec{q}} \simeq \frac{v_{\vec{q}}}{q}\Pi_1(\vec{q}, \omega_{\vec{q}}), \tag{3.88}$$

where $\Pi = \Pi_0 + i\Pi_1$ and

$$v_{\vec{q}} = \frac{\partial \omega_{\vec{q}}}{\partial q} = q\omega_{\vec{q}}^{-1}\left[1 + \frac{1}{2\omega}\frac{\partial \Pi_0(\vec{q}, \omega)}{\partial \omega}\right]^{-1}_{\omega=\omega_{\vec{q}}} \tag{3.89}$$

is the group velocity of the pion wave.

Since the effects of the medium are assumed to be small in setting up Eq. (3.88), we can use the low-density estimate,[46]

$$\Pi(\vec{q}, \omega_{\vec{q}}) \simeq 4\pi n_0 f_{\text{coh}} = \frac{4\pi n_0}{3} q^2 \sum_\alpha v_\alpha \overset{0}{h}_\alpha(\omega) \tag{3.90}$$

that follows from Eqs. (3.47) and (3.23) if we ignore the variation of f_{coh} with density. The imaginary part,

$$\Pi_1(\vec{q}, \omega_{\vec{q}}) = \frac{4\pi n_0}{3} q^2 \sum_\alpha v_\alpha \operatorname{Im}\overset{0}{h}_\alpha(\omega) \tag{3.91}$$

has two limiting forms, depending on the relative magnitude of q and p_F. At high wave numbers, $q \gg p_F$, one has the optical theorem[47]

$$4\pi q/3 \sum_\alpha v_\alpha \operatorname{Im}\overset{0}{h}_\alpha(\omega) = \tfrac{1}{2}[\sigma(\pi^- p) + \sigma(\pi^- n)] \equiv \bar{\sigma}, \tag{3.92}$$

where $\bar{\sigma}$ is the average πN cross section. Consequently

$$\Pi_1(\vec{q}, \omega_{\vec{q}}) \simeq n_0 \bar{\sigma} q, \quad q \gg p_F, \tag{3.93}$$

a result that coincides exactly with the impulse-approximation estimate of the imaginary part. The estimate (3.93) then combines with $1/\tau$ to give us the standard relation

$$\frac{1}{\lambda} = \frac{1}{v_{\vec{q}}\tau} = n_0 \bar{\sigma} \tag{3.94}$$

for the mean free path λ of a pion moving through a density n_0 of scatterers with a collision cross section σ per scatterer. Note that no Pauli principle effects occur in either of the above equations, as is to be expected for high-momentum collisions. By contrast, Pauli-principle effects dominate at low momenta, forcing Π_1 to vanish for $q < \frac{1}{2}p_F$. We pick up this effect to leading order in the density if we replace $\operatorname{Im}\overset{0}{h}_\alpha(\omega)$ by $\operatorname{Im}h_\alpha(\omega)$ in Eq. (3.91) and then use Eq. (3.43). The forms given for $\operatorname{Im}I_{\alpha\alpha}$ in Eqs. (3.32) are still valid if we replace p by q, ω by $\omega_{\vec{q}}$ in those equations, where $\omega_{\vec{q}} = (q^2 + \mu^2)^{1/2}$. This amounts to dropping the correction Π_0 to $\omega_{\vec{q}}$ in Eq. (3.88) in accord with the low-density limit. A direct calculation shows that

$$\Pi_1(\vec{q}, \omega_{\vec{q}}) \simeq \frac{4\pi n_0}{3} q^2 p_F \tilde{\mu}(\omega_{\vec{q}} - \tilde{\mu}) \times[(b_{11}^2 + 2b_{13}^2) + 3(b_{31}^2 + 2b_{33}^2)] \tag{3.95}$$

near the modified threshold $\omega = \tilde{\mu}$, where we set $h_\alpha(\tilde{\mu}) = b_\alpha$. The linear behavior of Π_1 with $\omega_{\vec{q}}$ near $\omega_{\vec{q}} = \tilde{\mu}$ is clearly visible in Fig. 14, which shows how one of the component functions, $\operatorname{Im}h_{33}(\omega) \equiv \operatorname{Im}h(\omega)$ of Π_1, vanishes at $\omega_q = \tilde{\mu}$. Numerically, one expects the b_α to be close to the (quenched) values of the free πN scattering volumes $h_\alpha(\mu)$ as determined by Eq. (3.77). Figure 13 illustrates the point for b_{33}. One sees that $h_{33}(\mu) = 0.160$ versus $h_{33}(\tilde{\mu}) \equiv b_{33} = 0.156$ at $\tilde{\mu} = 1.23\mu$, all in units of μ^{-3}, to be compared with the free πN scattering volume[38] of $C_{33} = 0.201(1/\mu^3)$.

The dispersion law (2.9) can also be cast with the form of a one-particle wave equation[47] for the pion, containing a pseudopotential[48] $v(\vec{r}, -i\vec{\nabla})$:

$$[\nabla^2 + p^2 - v(\vec{r}, -i\vec{\nabla})]\Phi(\vec{r}) = 0 \tag{3.96}$$

for a pion of incident wave number p. The pseudopotential is given by

$$v = v_R - iv_I = -\Pi_0[\rho(\vec{r}), -i\vec{\nabla}; \omega] - i\Pi_1[\rho(\vec{r}), -i\vec{\nabla}, \omega], \tag{3.97}$$

where $\rho = \rho(\vec{r})$ is the local nucleon density in the nucleus. Note that the pseudopotential is expected to be nonlocal and energy-dependent. These features are familiar from the related problem of constructing nucleon-nucleus potentials.[49] The energy dependence of v arises from the elimination of all nonelastic pion-nucleus channels in constructing the wave equation (3.96), or seen from our viewpoint, in constructing the propagator $D(\vec{q}, \omega)$. The nonlocal nature of v is specified by the p-wave nature of the basic πN interaction in our case. To see how this works, we look at v at low and high wave numbers. At low wave numbers, $q \ll p_F$, v is essentially real. Using Eqs. (3.90), (3.50), and (3.55) one has

$$v \simeq -\frac{4\pi n_0}{3} q^2 \sum_\alpha v_\alpha C_\alpha \to 4\pi\left(\frac{C_n + C_p}{2}\right)(\vec{\nabla} \cdot \rho\vec{\nabla}) \tag{3.98}$$

that is just the finite-nucleus version of the first term in the Ericson-Ericson result (3.57). Note that the operator equivalent of $q^2 n_0$ has been taken as $-\vec{\nabla} \cdot \rho(\vec{r})\vec{\nabla}$. One could equally well use the fully symmetrized version $-\frac{1}{4}[\rho\nabla^2 + 2\vec{\nabla} \cdot \rho\vec{\nabla} + \nabla^2\rho]$ or the purely local form $-\nabla^2\rho(\gamma)$.

At high wave numbers, the distinction between $\vec{q}$

and its operator equivalent is unimportant. We find

$$v - \frac{4\pi\rho(r)}{3} p^2 \sum_\alpha v_\alpha \mathrm{Re}\overset{0}{h}_\alpha(\omega) - i\rho(\vec{r})\bar{v}(\omega)p \qquad (3.99)$$

after setting $q \simeq p \gg p_F$, in agreement with the impulse approximation again.[47]

It should be pointed out that the absence of an imaginary part in Eq. (3.98) does *not* mean that the low-energy pion optical potential is real. The inclusion of π-$2N$ processes contributes an imaginary part in order n_0^2 down to zero pion momentum.[26]

H. Pion Mass Renormalization

The dispersion law (2.9) can also be written as

$$\omega^2 = q^2(1-\alpha) + \mu^2 , \qquad (3.100)$$

since $\Pi(\vec{q}, \omega) = q^2\,\alpha(\omega)$ in view of Eqs. (3.46) and (3.63). The interpretation of Eq. (3.100) as a relation determining the complex energy of the pion as a function of a given wave number (quasiparticles) has been discussed in the previous section.

On the other hand, the scattering of pions requires that we treat the energy ω as given[50] and determine the wave number $\vec{q}$ of the pion in the medium via Eq. (3.100). Since $\alpha(\omega) = \alpha_0 + i\alpha_1$ is complex, so is $\vec{q}$. Consequently we write $q = k(1+i\kappa)$, $n = n_0(1+i\kappa)$, and find that

$$\omega^2 = \frac{k^2}{n_0^2} + \mu^2 ; \quad n^2 = \frac{1}{1-\alpha_0 - i\alpha_1} . \qquad (3.101)$$

The n_0^2 factor in the denominator shows that the pion speed (group velocity) is decreased in the nuclear medium by the self-energy $q^2\,\alpha(\omega)$, if $\alpha > 0$, even though the pion wave number k is increased in the medium. One sees this directly from the expression for the group velocity $v_g = \partial\omega/\partial k$ of the pion wave. According to Eq. (3.101), one has

$$v_g = \frac{k}{\omega n_0^2} = \frac{p}{n_0\omega} \qquad (3.102)$$

in the medium, which is slower by a factor n_0 than the group velocity p/ω in free space. This curious effect, which runs contrary to intuition, comes about because a self-energy of the momentum-dependent form $q^2\,\alpha(\omega)$ "dresses" the free pion in a way which at low energies can be described by giving the pion an effective mass $\mu^* = n_0^2\mu$ that is *larger* than its mass in free space. This is to be contrasted with the case of an attractive and momentum-independent potential, for which both the wave number and the group velocity increase in the medium, and for which there is no modification of mass. As an added check on our interpretation of Eq. (3.100) as determining a complex wave number q for real ω, we note the property (λ is the mean free path as before)

$$\frac{\lambda}{v_g} = \frac{1}{2k\kappa}\frac{n_0^2\omega}{k} \simeq \frac{\omega}{\alpha_1 k^2} , \qquad (3.103)$$

since for small absorption coefficients $2\kappa \simeq \alpha_1 n_0^2$. However, $\omega/(\alpha_1 k^2)$ is just the quasiparticle lifetime τ of Eq. (3.88) as calculated for the specific dispersion law (3.100). Thus we regain the relation $\lambda \simeq v_g\tau$ by another method.

IV. APPLICATIONS

A. Chew-Low Solution

Before proceeding to the problem of pion-nucleus scattering, we investigate to what extent the Chew-Low model describes πN scattering in the (3, 3) resonance region. To this end we adopt the framework of the static Chew-Low theory that was reviewed in Sec. III A. The basic equation in that theory is given by (3.11). If we restrict our attention to the (3, 3) amplitude $\overset{0}{h}_{33}(\omega) = \overset{0}{h}(\omega)$ only, and neglect the crossing terms, we are left with

$$\overset{0}{h}(\omega) = \frac{\overset{0}{\lambda}}{\omega} + \frac{1}{\pi}\int_\mu^\infty d\omega_{\vec{p}}\, p^3 v^2(p) \frac{|\overset{0}{h}(\omega_{\vec{p}})|^2}{\omega_{\vec{p}} - \omega - i\delta} , \qquad (4.1)$$

where $\overset{0}{\lambda} = \frac{4}{3} f_r^2/4\pi\mu^2$. The explicit solution of Eq. (4.1) has been given in Eqs. (3.60)–(3.62). Since the coupling constant $\overset{0}{\lambda} \simeq 0.11\mu^{-2}$ is known, the only remaining parameter is the high-momentum cutoff in $v^2(p)$. This admittedly *ad hoc* feature is unavoidable in a theory using point nucleons. We have employed two forms for $v^2(p)$: (i) a Gaussian

$$v^2(p) = \exp\left(-\frac{p^2}{p_0^2}\right) \qquad (4.2)$$

and (ii) a sharp cutoff

$$v^2(p) = \begin{cases} 1 & p \le p_0 \\ 0 & p > p_0 \end{cases} \qquad (4.3)$$

in order to get some feeling for the effect of varying the form of $v^2(p)$. In each case p_0 can be adjusted to fit the peak in the experimental πN cross section. We have used the $\pi^+ p$ data of Carter *et al.*[5] These authors parametrize $\overset{0}{h}$ as

$$\overset{0}{h}(\omega_\kappa) = \frac{\Gamma(\omega_\kappa)}{2\kappa^3} \frac{1}{\omega_0 - \omega_\kappa - (i/2)\Gamma(\omega_\kappa)} \qquad (4.4)$$

taking a constant value $\omega_0 = 1.904\mu$ for the resonance energy, but an energy-dependent width

$$\Gamma(\omega_\kappa) = \frac{4m\kappa^3 a^3 \gamma^2 \mu}{(\omega_0 + \omega_\kappa)(1+\kappa^2 a^2)} . \qquad (4.5)$$

Here m = proton mass, $a = 0.6277\mu^{-1}$, $\gamma^2 = 0.1709$, while κ and ω_κ are the pion momentum and total energy in the πN center-of-mass system, as before. The parametrization (4.4) has the same

form as our equation (3.60) (as must any unitary amplitude) except that ω_0 is now taken as constant, while the width $\Gamma(\omega)$ in Eq. (4.5) is damped at high energies relative to the Chew-Low result (3.61).

For the Gaussian cutoff of Eq. (4.2), a value $p_0 = 13.8\mu$ correctly positions the (3,3) resonance at 173.9-MeV lab kinetic energy while a value $p_0 = 11.75\mu$ is required for the sharp cutoff model.[51] The predictions of the Chew-Low model with a Gaussian (G) and sharp cutoff (SC) are shown in Fig. 11, together with the experimental points,[5] and the fit (C) obtained using Eqs. (4.4) and (4.5). One notices that the peak in the cross section occurs at an energy below 188.3 MeV (the lab kinetic energy corresponding to ω_0) due to the energy dependence in $\Gamma(\omega_\kappa)$ as well as the wavelength factor $\lambda\!\!\!^{-2} = \kappa^{-2}$ in the cross section. The other feature to note is that the Chew-Low model gives a resonance curve which is overly skewed toward high energies. This is because the Chew-Low width parameter $\Gamma(\omega)$ is too large at high energies in comparison to the $\Gamma(\omega)$ of Eq. (4.5), or other phenomenological forms.[7]

One sees from Fig. 11 that the results for different cutoff functions are essentially the same. Therefore, we restrict ourselves in the following to the sharp cutoff of Eq. (4.3), which is numerically more convenient. Using Eq. (4.3), one can calculate the resonance parameter ω_0 from Eq. (3.62) as

$$\frac{1}{\omega_0} = \frac{\lambda\!\!\!^{0}}{\mu}\left[\frac{(\tilde{M}^2-1)^{1/2}}{\tilde{M}\omega}(\tilde{M}\omega-1) - \frac{1}{\omega^2}\cos^{-1}\left(\frac{1}{\tilde{M}}\right) + \cosh^{-1}(\tilde{M}) - \frac{(\omega^2-1)^{3/2}}{\omega^2}\ln\left|\frac{(\tilde{M}-1)^{1/2}(\omega^2-1)^{1/2}+\tilde{M}\omega-1}{(\tilde{M}-\omega)}\right|\right] \tag{4.6}$$

if $\omega > 1$, where we have expressed all energies in units of μ. Here $\tilde{M} = (p_0^2+1)^{1/2} \simeq 11.8$ is the cutoff mass.

The effective-range expansion of Chew and Low uses the "soft-pion limit" of ω_0 at $\omega = 0$. A direct calculation gives

$$\frac{1}{\omega_0(0)} = \frac{\lambda\!\!\!^{0}}{\mu}\left[(\tilde{M}^2-1)^{1/2}\left(1+\frac{1}{2\tilde{M}^2}\right) - \tfrac{3}{2}\cos^{-1}\left(\frac{1}{\tilde{M}}\right)\right] \simeq \frac{1}{3\mu} \tag{4.7}$$

for $\lambda\!\!\!^{0} = 0.11\mu^{-2}$, a result which is inconsistent with the required value $\omega_0 \simeq 2\mu$ in the energy range 1.5–2μ around the (3,3) resonance. This inconsistency is again connected with the neglect of the crossed channels. However, ω_0 is a slowly varying function of ω in the region of interest, see Fig. 16, so that its replacement by a constant is a good approx-

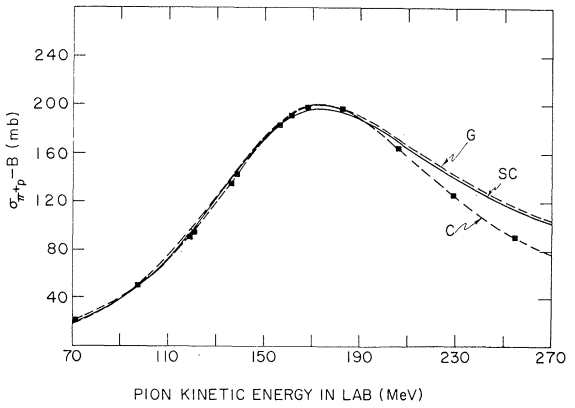

FIG. 11. The total π^+p cross section σ_{π^+p} [minus a small background B from channels other than (3,3)] as a function of pion lab kinetic energy. The dashed curve labeled G corresponds to the Chew-Low prediction using the Gaussian cutoff of Eq. (4.2) with $p_0 = 13.8\mu$. The solid curve labeled SC represents the Chew-Low result with the sharp cutoff of Eq. (4.3), using $p_0 = 11.75\mu$. Both curves use a renormalized coupling constant $f_r^2/4\pi = 0.08$. The dashed curve labeled C is the fit of Ref. 5, using Eqs. (4.4)–(4.5). The experimental points of Ref. 5 are shown as black squares. The experimental errors are not larger than the size of the squares.

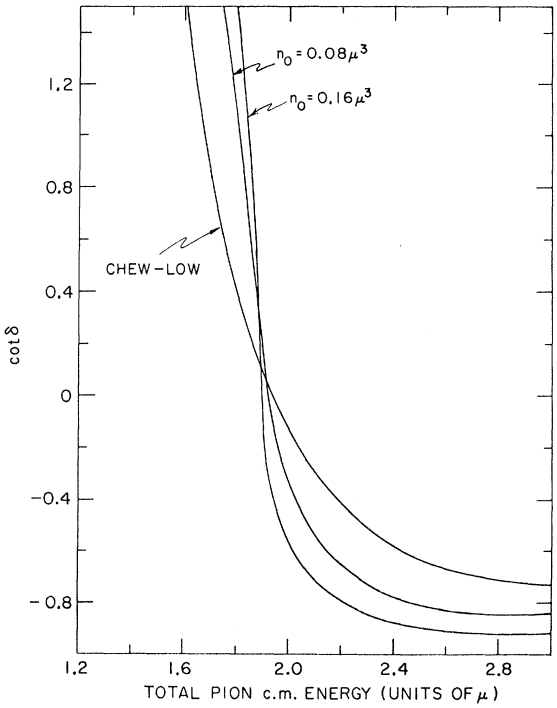

FIG. 12. The phase shift $\cot\delta(\omega)$ as a function of the total pion c.m. energy ω for densities $n_0 = 0.08\mu^3$ and $0.16\mu^3$. The zero-density Chew-Low phase shift is also shown for comparison. These curves correspond to the iterative solution of Eq. (3.82).

imation. We simply note that this constant is not given by Eq. (4.7).

B. Iterative Solution of the Chew-Low Equation in the Nuclear Medium

We have pointed out that the condition of small pion wavelength relative to the internucleon spacing ($\lambda\!\!\!^{-}/r_0 \ll 1$) (for a low-density treatment to apply) is not well satisfied in the (3, 3) resonance region for actual nuclear densities. One has therefore to attempt a nonperturbative solution of Eq. (3.78) for $h(\omega)$. We have found that the following procedure converges rapidly: Start with some small density $n_0 = n_0^{(0)}$ and substitute an initial guess $h^{(0)}(\omega)$ for $h(\omega)$ into Eq. (3.76) for the effective coupling constant λ'. The quantities on the right-hand side of Eq. (3.78) can then be computed and a first iterate $h^{(1)}(\omega)$ found for $h(\omega)$. For $\omega > \tilde{\mu}$, it is in fact more convenient to use Eq. (3.82) and construct $h^{(1)}(\omega)$ from a knowledge of the phase shift δ plus unitarity. The process is then repeated until self-consistency is obtained. Knowing a solution for $h(\omega)$ at a given density, one uses *this* solution as the initial guess for the next density $n_0^{(1)} = n_0^{(0)} + \Delta n_0$, etc. For sufficiently small Δn_0, the convergence is rapid at each density, and one obtains a complete survey of $h(\omega)$ as a function of energy and density in this fashion. Calculations have been carried out in the density range $0 \leq n_0 \leq 0.48\mu^3$, and an energy grid $\Delta\omega = 0.02\mu$ (about 4 to 5 MeV in lab kinetic energy) in the range $\mu \leq \omega \leq 5\mu$. A coarser grid $\Delta\omega = 0.04\mu$ was used for $\omega > 5\mu$. Tests were also made using a finer grid $\Delta\omega = 0.01\mu$, but this produced a negligible change in the final results for $h(\omega)$. At fixed energy ω, the amplitude $h(\omega)$ varies slowly with density, so not many grid points are needed for the n_0 integration that determines the pion self-energy.

The iteration procedure based on Eqs. (3.78) and (3.82) converges rapidly for $0 \leq n_0 \leq 0.2\mu^3$, i.e. up to one half of the density of nuclear matter. A maximum of eight iterations is required to obtain self-consistency in $h(\omega)$ to one part in 10^{-3} to 10^{-6} depending on the value of ω. In most cases, three to five iterations are sufficient. A *single* iteration of Eq. (3.78) is generally not adequate, however. In all cases, the $h(\omega)$ which results from the iterative procedure is substituted back into Eq. (3.59), and the right-hand side is compared to the left-hand side at each ω. For each n_0, the two sides of this equation agreed to within 0.1%, and usually much less, confirming that a self-consistent solution had been obtained numerically. The simplified version of Eq. (3.59) with $\tilde{I}(\omega)$ replaced by its low-energy limit $\tilde{I}(\mu) = N_0$ was also solved numerically for comparison. In this case the convergence is even more rapid. Finally, we remark that convergence becomes slower in both cases as the density increases.

In Figs. 12–16 we show a few sample results of the numerical calculations. Figure 12 displays the cotangent of the phase shift[52] δ, as a function of ω, obtained by solving Eq. (3.82). We show the Chew-Low (zero-density) phase shift for comparison. In the resonance region, the finite-density phase shift changes more rapidly than the Chew-Low limit, indicating a sharper resonance in the

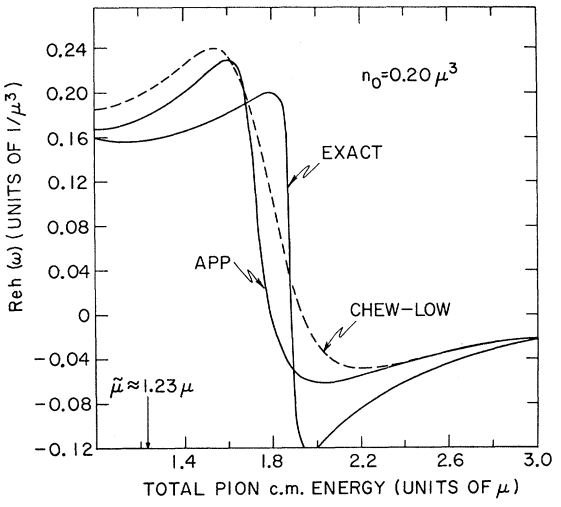

FIG. 13. Real part of the effective pion-nucleon amplitude $h(\omega)$ as a function of ω for density $n_0 = 0.20\mu^3$. The curve labeled EXACT refers to the solution of Eq. (3.59) while APP labels the solution of Eq. (3.59) with the approximation $\tilde{I}(\omega) \approx \tilde{I}(\mu) = N_0$. The Chew-Low result is shown for comparison (dashed line).

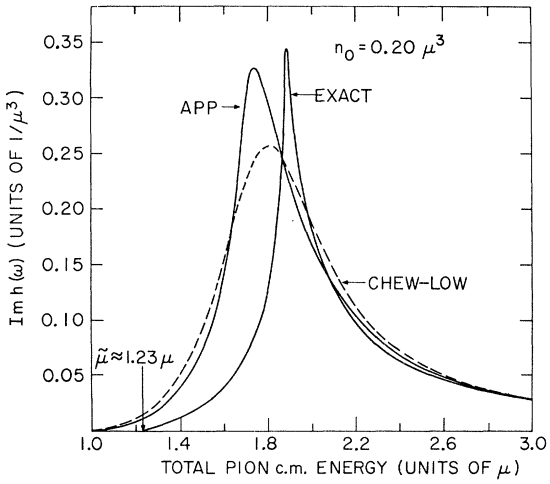

FIG. 14. Imaginary part of $h(\omega)$ as a function of ω for $n_0 = 0.20\mu^3$. The curves are labeled as in Fig. 13. The modified threshold $\tilde{\mu}$ is indicated by an arrow.

cross section. We have already anticipated this result in connection with Eq. (3.80), which shows the narrowing of the (3,3) resonance in nuclear matter by Pauli-principle effects. The energy at which δ passes through $\pi/2$ [$\cot\delta(\omega)=0$] decreases slightly as n_0 increases.

In Figs. 13 and 14, we exhibit the real and imaginary parts of $h(\omega)$ at a density of $0.2\mu^3$, and compare these to both the Chew-Low amplitude given by Eq. (3.60), as well as the solution of Eq. (3.59) with $\tilde{I}\simeq\tilde{I}(\mu)=N_0$. The latter approximation is seen *not* to provide a good approximation to the exact solution of Eq. (3.59), except at high energies, where all three amplitudes become equal. As seen from Figs. 9 and 10, the approximation $\tilde{I}\simeq\tilde{I}(\mu)$ is actually quite poor in the resonance region ($1.5\mu \leq \omega \leq 2\mu$) where $\tilde{I}(\omega)$ is typically of order 2–2.5 times $\tilde{I}(\mu)$. The imaginary part of $\tilde{I}(\omega)$ is also of the same order as the real part in the resonance region, a feature that the approximation $\tilde{I}(\omega)\simeq\tilde{I}(\mu)$ ignores entirely. In addition, $\mathrm{Im}\tilde{I}$ is responsible for the upward shift of the threshold from μ to $\tilde{\mu}$.

The shift in peak energy is shown in Fig. 14, which gives $\mathrm{Im}h(\omega)$ as a function of ω at a density $n_0=0.2\mu^3$. We see that the peak in $\mathrm{Im}h(\omega)$ has been shifted *upward* in energy by the presence of the medium and appears appreciably narrowed. Thus a modified π^+p "cross section" $\sigma_{\pi^+p}=8\pi p \times \mathrm{Im}h(\omega)$ would display a resonance at a higher energy with a smaller width than the basic Chew-Low resonance.[53] This feature is a direct result of the quenching of the effective coupling constant λ' as per Eq. (3.76). A reduced value of the coupling moves the resonance energy upward (since ω_0' is inversely proportional to λ'). We have already discussed the narrower width in terms of Pauli-principle restrictions.

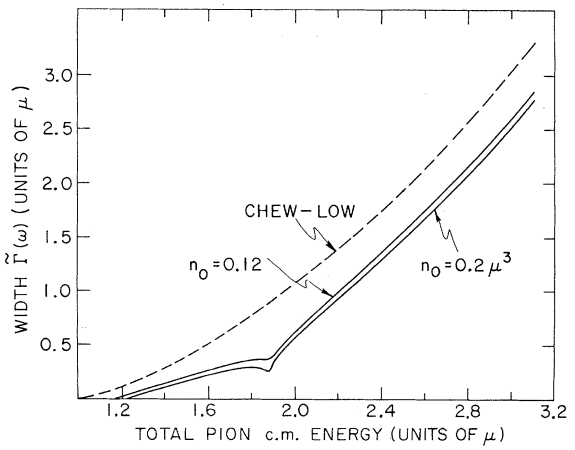

FIG. 15. The width function $\tilde{\Gamma}(\omega)$ of Eq. (3.80) as a function of ω for $n_0=0.12\mu^3$ and $0.2\mu^3$. The Chew-Low width $\Gamma(\omega)$ of Eq. (3.61) is shown for comparison.

The width functions $\tilde{\Gamma}(\omega)$ and $\Gamma(\omega)$ given by Eqs. (3.80) and (3.61) are shown in Fig. 15 as a function of ω. The reduction of $\tilde{\Gamma}(\omega)$ relative to $\Gamma(\omega)$, as well as its smooth dependence on density, is illustrated by the curves at densities $n_0=0.12\mu^3$ and $n_0=0.2\mu^3$. In Fig. 16, we compare the modified resonance energy $\tilde{\omega}_0$ of Eq. (3.81) with the Chew-Low resonance energy ω_0 of Eq. (3.62). The same curve also shows the approximate value of $\tilde{\omega}_0$ if we assume $\tilde{I}\simeq\tilde{I}(\mu)$ for all ω. We note that $\tilde{\omega}_0$ varies more rapidly than ω_0, and that $\tilde{\omega}_0>\omega_0$ in the region of ω that lies below the peak value of $\mathrm{Im}h(\omega)$.

C. Numerical Results

In this section we show some typical results for the pion self-energy $\Pi(q)$, as well as examples of the refractive index $n(\omega)$ and the mean free path of pions in nuclear matter. The self-energy is obtained by combining Eqs. (3.58) and (3.23) in the form

$$\frac{\Pi(q)}{q^2}=\frac{16\pi}{3}\int_0^{n_0} dn_0' h(\omega,n_0') \tag{4.8}$$

and then carrying out the integration over density numerically. The results are shown in Figs. 17 and 18. The first-order result obtained by replacing $h(\omega)$ by the Chew-Low amplitude $\overset{0}{h}(\omega)$ is also shown for comparison. We observe that the real part of $\Pi(q)$ is generally diminished by the presence of the medium, in agreement with the quenching effect discussed previously. Also, the peak value of $\mathrm{Im}[q^{-2}\Pi(q)]$ has been shifted up in energy and narrowed in width relative to the Chew-Low

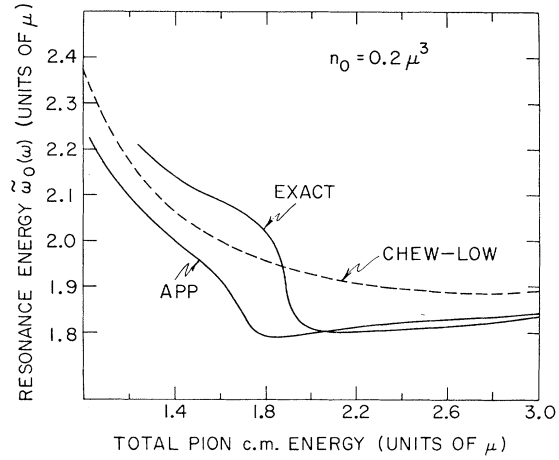

FIG. 16. The modified (3,3) resonance energy $\tilde{\omega}_0(\omega)$ as a function of ω for $n_0=0.2\mu^3$. The curve labeled EXACT corresponds to Eq. (3.81) while curve APP refers to the approximation $\tilde{I}(\omega)\approx\tilde{I}(\mu)$ as in Fig. 13. The Chew-Low resonance energy $\omega_0(\omega)$ of Eq. (3.62) is also shown for comparison (dashed curve).

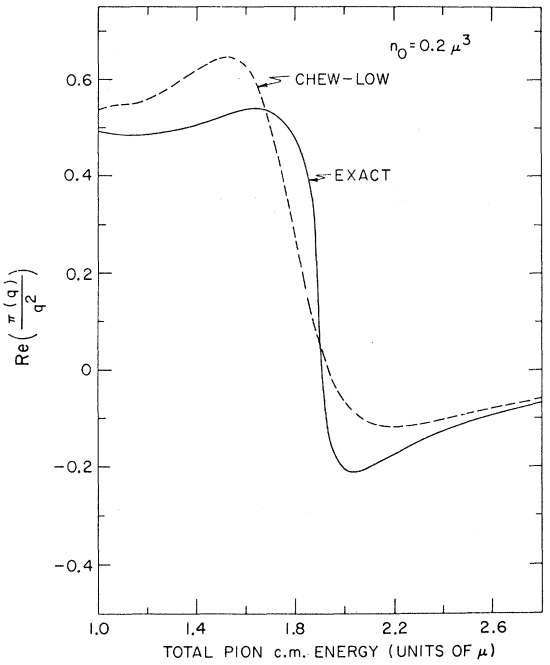

FIG. 17. Real part of the pion self-energy $\Pi(\vec{q},\omega)/q^2$ as a function of energy for $n_0 = 0.2\mu^3$. The solid curve refers to the exact calculation using Eq. (4.8). The dashed curve represents the first-order approximation to $\Pi(q)$.

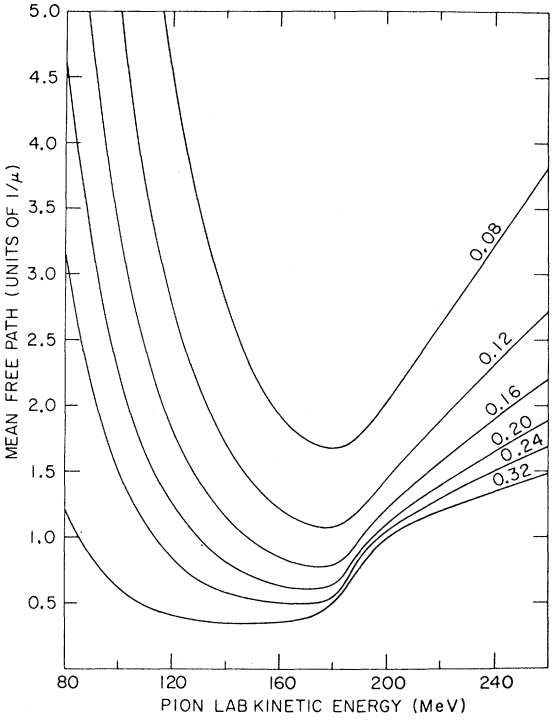

FIG. 19. Pion mean free path $\lambda(\omega)$ as a function of energy for various values of the density n_0 (labeled at right of figure in units of μ^3). These curves are based on the solution of Eq. (3.59) for $h(\omega)$.

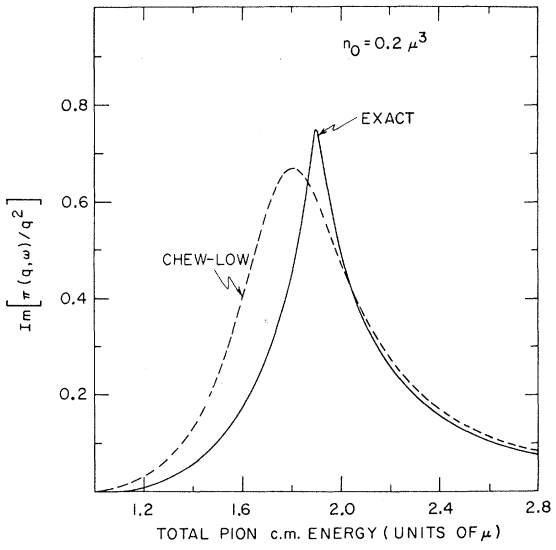

FIG. 18. Imaginary part of $\Pi(\vec{q},\omega)/q^2$ as a function of ω for a density $n_0 = 0.2\mu^3$. The solid curve is obtained from Eq. (4.8). The dashed curve is the first-order Chew-Low approximation.

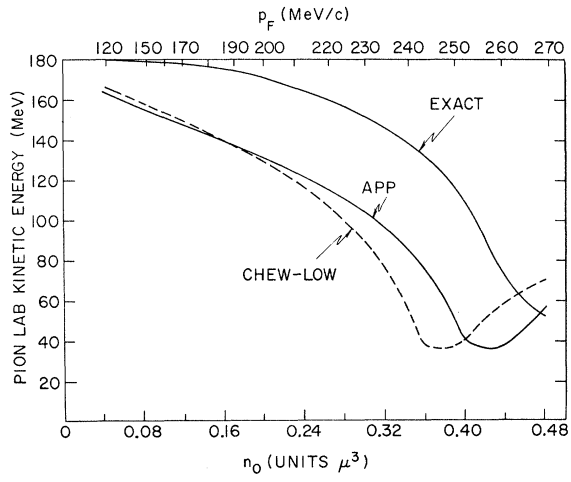

FIG. 20. Pion kinetic energy (MeV) for which the mean free path $\lambda(\omega)$ has its minimum value, as a function of the density n_0. The curve labeled EXACT is obtained by solving Eq. (3.59) while curve APP corresponds to using $I(\omega) \approx I(\mu)$, as in Figs. 13 and 16. The dashed curve is the first-order Chew-Low approximation.

solution. This is just the reflection of the same effects in $\mathrm{Im}h(\omega)$ as per Eq. (4.8).

A knowledge of $\alpha = q^{-2}\Pi(q)$ determines the refractive index $n(\omega)$ of nuclear matter from Eq. (3.65′). In turn, the imaginary part of $n(\omega)$ determines the mean free path of pions of momentum p and energy $\omega = (p^2+\mu^2)^{1/2}$ as in Eq. (2.12):

$$\frac{1}{\lambda(\omega)} = 2p\,\mathrm{Im}n(\omega)\,. \tag{4.9}$$

The mean free path obtained from the numerical integration of Eq. (4.8) to determine α is shown in Fig. 19, for various final densities n_0. The next figure (Fig. 20) shows the energy for which $\lambda(\omega)$ assumes its minimum value as a function of the density. The energy dependence of the mean free path reflects itself directly in the total absorption cross section for pions in nuclear matter. In order to calculate σ_{abs} we treat the nucleus as an opaque sphere of radius R and uniform density n_0. Then according to the classical optical-model formula,[47]

$$\sigma_{\mathrm{abs}} = \pi R^2(1-T)\,, \tag{4.10}$$

where the transmission coefficient T is given by

$$T = \frac{\lambda^2}{2R^2}\left[1-\left(1+\frac{2R}{\lambda}\right)\exp\left(-\frac{2R}{\lambda}\right)\right]. \tag{4.11}$$

One finds that the peak value in σ_{abs} occurs very close to the *minimum* value of $\lambda(\omega)$. This is seen immediately if $\lambda \gg R$ by expanding $1-T \simeq \frac{4}{3}R/\lambda$. In realistic cases λ/R is generally small rather than large near a minimum value of λ, but this does not appreciably alter the qualitative nature of the result. Thus if we adopt Eq. (4.10), Fig. 20 may be interpreted as a plot of the (3,3) resonance energy in nuclei as a function of the nuclear density.

The results shown in Fig. 20 emphasize the large difference between the predictions of the first-order estimate $h(\omega) \simeq \overset{0}{h}(\omega)$ for determining the mean free path (broken curve) and the exact calculation. The first-order Chew-Low model[20] predicts resonance energies that are consistently 30–60 MeV *below* those following from the complete calculation. Thus the error incurred in using the first-order multiple-scattering approximation to $\Pi(q)$ is of the same order as the energy shift one is trying to understand. This suggests a poor convergence of the multiple-scattering approximation near the (3,3) resonance. Other authors have arrived at similar conclusions.[14,15]

We also note that our calculation predicts that the π-nucleus (3,3) resonance energy decreases with increasing density up to a certain critical density and then starts to increase again. On the other hand, the discussion of Sec. B above showed that the basic resonance energy in $\mathrm{Im}h(\omega, n_0)$ *increases* with increasing n_0. Thus we have two competing energy-shift mechanisms in π-nucleus scattering: (i) an *upward* shift due to the quenching of the πN coupling constant by the medium [Eq. (3.76)] and (ii) a *downward* shift due to dispersive effects in the medium [Eq. (3.66)]. Since quenching is absent in the first-order calculation, the corresponding minimum in $\lambda(\omega)$ always lies below the exact result as long as n_0 is below a certain critical density ($n_0 \lesssim 0.44\mu^3$ in the first-order calculation and somewhat higher in the exact calculation). Above this density, the resonance energy again increases. This effect comes about from

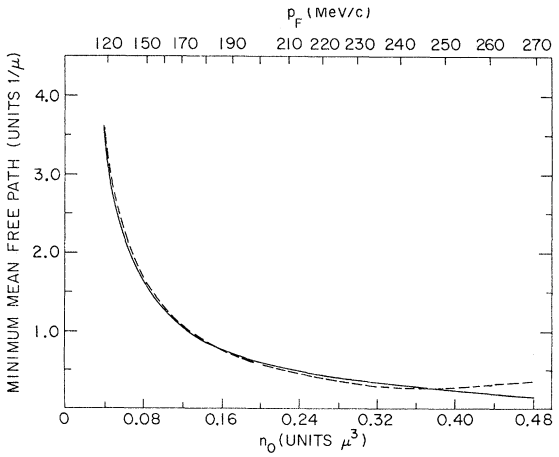

FIG. 21. Minimum value λ_{min} of the pion mean free path as a function of the density n_0. The solid curve represents the result of solving Eq. (3.59), while the dashed curve corresponds to the first-order approximation to $h(\omega)$.

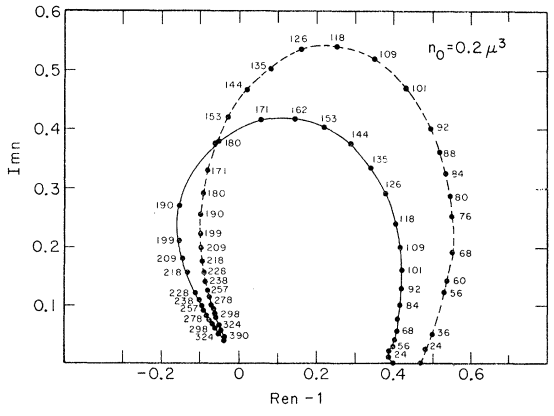

FIG. 22. Trajectory of the pion index of refraction $n(\omega)$ as a function of ω for $n_0 = 0.2\mu^3$. The solid curve represents the exact calculation, while the dashed curve corresponds to the first-order Chew-Low approximation. The curves are labeled by the value of the pion lab kinetic energy at each point.

the energy dependence in the shift function $\Delta(\omega_\kappa)$ given by Eq. (3.67). If we write

$$\Delta(\omega_\kappa) = \Delta_0 \frac{\omega_0}{\omega_\kappa}, \tag{4.12}$$

where $\Delta_0 = 16\pi n_0 \overset{0}{\lambda}\eta/3$ is the value of Δ at $\omega = \omega_0$, and assume that the deviation from unity of the refractive index n_{CL} in Eq. (3.66) is small, then

$$(n_{\mathrm{CL}} - 1) \simeq \frac{\Delta_0}{2\omega_0} \frac{1}{[s - s^2 - (\Delta_0/\omega_0)] - i(\overset{0}{\lambda}\kappa^3/\omega_0)} \tag{4.13}$$

with $s = \omega_\kappa/\omega_0$. The imaginary part of this expression determines the mean free path as

$$\frac{1}{\lambda(s)} = \frac{p\Delta_0}{\omega_0} \frac{(\overset{0}{\lambda}\kappa^3/\omega_0)}{[s - s^2 - (\Delta_0/\omega_0)]^2 + (\overset{0}{\lambda}\kappa^3/\omega_0)^2}, \tag{4.14}$$

where p is the pion momentum in the lab, $p = \kappa\eta^{-1}$. The minimum value of $\lambda(s)$ occurs approximately at the larger root of $s - s^2 - (\Delta_0/\omega_0) = 0$ or

$$s = \tfrac{1}{2} + \tfrac{1}{2}[1 - 4(\Delta_0/\omega_0)]^{1/2} \tag{4.15}$$

provided that this root is real. Since Δ_0/ω_0 is proportional to the density, this root moves down with increasing density until it reaches its limiting value $s = \frac{1}{2}$ for $4\Delta_0 = \omega_0$. Using the values $\omega_0 = 2.17\mu$, $\overset{0}{\lambda} = 0.11\mu^{-2}$, and $\eta \simeq 0.87$ near resonance ($s \simeq 1$) one finds that $4\Delta_0 \simeq 3\omega_0 n_0$ in units of μ^{-3}, so that the critical density is of order $n_0 \simeq \frac{1}{3}\mu^3$, in agreement with the broken curve in Fig. 20. When $4\Delta_0$ exceeds ω_0, the minimum value of $\lambda(s)$ would occur at $s = \frac{1}{2}$ independent of the density, were it not for the phase-space factor κ^3 that moves this maximum to higher energies in a fashion that depends on density because of the factor Δ_0 in the numerator of Eq. (4.14).

In Fig. 21, we plot λ_{min} as a function of density. We remark that the first-order and exact calculations of λ_{min} are very close, but the energies at which λ_{min} is reached are of course quite different. For $n_0 \geq 0.1\mu^3$, we see that λ_{min} is small compared to a typical nuclear radius, even for light nuclei. Near resonance, the absorption of pions is thus essentially a surface reaction, since the small mean free path prevents the pions from penetrating into the nuclear interior.

It is also interesting to plot trajectories of the real and imaginary parts of the refractive index $n(\omega)$, as in Fig. 22. One notices that the trajectory is of a smaller size for the exact calculation, which implies that the change in the real part of the wave number as the pion enters the medium is correspondingly smaller (for $\omega < \omega_0$). Once again, this exhibits the quenching effect of the medium on the basic (3, 3) resonance.

D. Absorption Cross Sections

The classical formula (4.10) for the absorption cross section neglects the wave nature of the incident particle in the scattering process. In particular, this formula assumes that the incident particle can be localized with arbitrary precision. It is well known from nuclear reaction studies with strongly absorbed incident particles that consid-

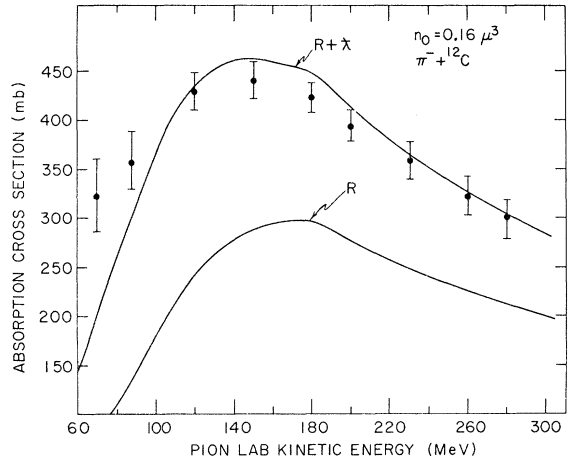

FIG. 23. Comparison of the absorption cross section σ_{abs} calculated classically (curve R) and with an energy-dependent effective radius (curve $R + \lambda$), both according to Eqs. (4.10)–(4.11). Both curves are for the reaction $\pi^- + {}^{12}C$ at a density $n_0 = 0.16\mu^3$. The experimental points are taken from Ref. 1.

TABLE I. Equivalent spherical radius R and bulk density ρ_{bulk} for various nuclei.

Nucleus	R (fm)	ρ_{bulk} (units μ^3)
^{4}He	2.16	0.268
^{6}Li	3.23	0.121
^{7}Li	3.11	0.157
^{12}C	3.18	0.255
^{16}O	3.55	0.241
^{28}Si	4.0	0.299
^{32}S	4.15	0.304
^{40}Ca	4.46	0.305
^{51}V	4.62	0.349
^{56}Fe	4.88	0.326
^{58}Ni	4.96	0.321
^{88}Sr	5.30	0.40
^{120}Sn	5.95	0.386
^{197}Au	6.84	0.415
^{208}Pb	7.05	0.401

erable improvement between theory and experiment results on replacing the nuclear radius in Eq. (4.10) by an effective radius $R' = R + \lambda\!\!\!^{-}$, where $\lambda\!\!\!^{-} = 1/p$ is the reduced wavelength of the pion.[54] The increase of the nuclear radius by a wavelength accounts in a very rough way for the lack of localization of the incident particle to better than its own wavelength. Hence, we use

$$\sigma_{abs} = \pi(R + \lambda\!\!\!^{-})^2[1 - T(R + \lambda\!\!\!^{-})] \tag{4.16}$$

in comparing with experimental data. The correction $R \to R'$ is particularly important for light nuclei where $\lambda\!\!\!^{-}$ is of the same order as the nuclear radius (in which event one should do a complete wave mechanical calculation anyway). Figure 23 shows the classical absorption cross section for $\pi^- + {}^{12}C$ scattering, with and without the wavelength correction, using a nuclear density of $n_0 = 0.16\,\mu^3$. The agreement with experiment is probably better than the crude formula (4.16) would justify. Qualitatively, the replacement $R \to R'$ has the effect of introducing an additional energy shift that moves the (3,3) resonance peak in σ_{abs} below the energy at which the mean free path is a minimum (the numbers are 149.3 versus 175.3-MeV lab kinetic energy in Fig. 23). Clearly a full quantum-mechanical calculation is necessary, based on the wave equation (3.96), before quantitative comparisons with experiment are really meaningful.

The acquisition of more extensive data at the Los Alamos Meson Physics Facility and other meson facilities should justify these more extensive calculations at a later stage. For the moment, we content ourselves with some semiquantitative predictions of the (3,3) resonance energy with mass

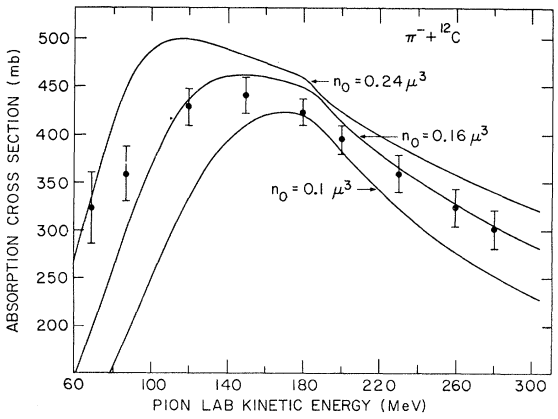

FIG. 24. Absorption cross sections σ_{abs} for $\pi^- + {}^{12}C$ at various densities n_0. An effective radius $R + \lambda\!\!\!^{-}$ was used in Eqs. (4.10)–(4.11) with $R = 3.18$ fm. The values of the mean free path $\lambda(\omega)$ are obtained by solving Eq. (3.59) for $h(\omega)$. The experimental points are taken from Ref. 1.

number A. To do so in the framework of the semiclassical formula (4.16), we require (i) a nuclear radius R and (ii) an effective density for nucleons in the nuclear surface. We obtain the former by averaging values of the equivalent charge radius[55] obtained from electron scattering. We then assume that neutrons occupy the same volume as protons and obtain $\rho_{bulk} = 3A/(4\pi R^3)$ for the bulk density. These values of R and ρ_{bulk} are tabulated in Table I. However, pion absorption takes place primarily in the nuclear surface, so it would be incorrect to equate the n_0 of our nuclear-matter calculation to ρ_{bulk}. Instead we use the observed peak position (145 ± 8 MeV) of the (3,3) resonance in $\pi^- + {}^{12}C$ scattering to determine n_0. Figure 24 shows calculated curves of σ_{abs} for $n_0 = 0.1$, 0.16, and $0.24\,\mu^3$. The choice $n_0 = 0.17\,\mu^3$ correctly positions the resonance peak at 145 MeV and at the same time reproduces the absolute absorption cross section above 100 MeV remarkably well. (A fit to the lower-energy data can only be undertaken in a model that also includes s-wave scattering.) The value $n_0 = 0.17\,\mu^3$ corresponds to

$$n_0 \simeq \tfrac{2}{3}\rho_{bulk} \tag{4.17}$$

for ${}^{12}C$. If we assume this prescription for all nuclei then the peak value of σ_{abs} varies with A as shown in Fig. 25. The general trend is towards lower energies as is to be expected, the local variations coming from nonsmooth changes in ρ_{bulk}. For instance, the classical model predicts very small shifts in ${}^6Li$ and ${}^7Li$, which are loosely

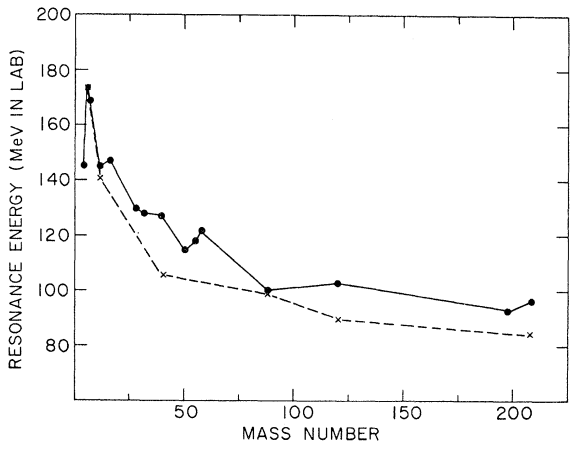

FIG. 25. Predicted (3,3) resonance energies as a function of mass number A of the target nucleus. The solid curve corresponds to using an effective density $n_0 = \frac{2}{3}\rho_{bulk}$, where the values of ρ_{bulk} are given in Table I. The broken curve uses densities ρ_{bulk} from Ref. 57. The 15 dots correspond to the nuclei listed in Table I. Connecting lines are drawn to guide the eye, and do not represent the results of calculations.

bound, but a larger shift[56] in ^{4}He. For nuclei heavier than mass number 80, the solid curve in Fig. 25 indicates that the resonance energy saturates at about 100 MeV.

An alternative to Eq. (4.17) is to use $\rho_{\text{bulk}} = 2p_F^3/3\pi^2$, and then adopt values of the Fermi momentum obtained from quasielastic electron scattering.[57] Except for ^{6}Li, these values are consistently larger than those following from the uniform model. The results obtained with this prescription are also shown in Fig. 25.

The relation (4.17) is of course a very qualitative one, and pion absorption on different nuclei could well sample different regions of the surface depending on the incident energy. In fact, in the uniform model it is probably more correct to determine the effective density from individual observed resonance positions than vice versa. As a qualitative guide, Fig. 26 shows how the resonance energy in ^{4}He, ^{12}C, and ^{208}Pb changes with density, assuming the validity of the semiclassical result (4.16) to compute the resonance energy. We remark again that these curves are of qualitative significance only and cannot replace a full-wave-mechanical calculation, especially in the case of light nuclei. The calculations we have described use a very simple model of the nucleus as a uniform sphere, so that no detailed nuclear structure or shell effects can appear. Strong deviations from the trend of energy shifts shown in Fig. 25 could be associated with effects of nuclear structure. But in any case we feel that the qualitative information in Fig. 25 should be of some use in planning systematic experiments in the (3, 3) resonance region.

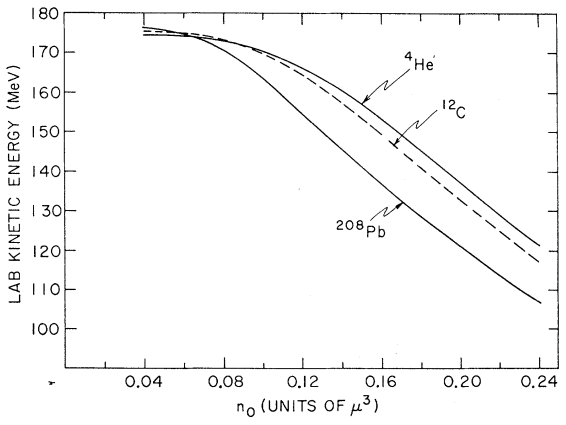

FIG. 26. The (3,3) resonance energy as a function of density n_0 for ^{4}He, ^{12}C, and ^{208}Pb. The charge radii of Table I were used in conjunction with Eqs. (3.59), (4.10), and (4.11).

V. SUMMARY

While most of the results and developments of the previous two sections are self-contained, it is useful to summarize the main procedures and physical assumptions used in this study of pion-nucleus interactions. We have based our approach on the construction of the pion self-energy $\Pi(q)$, which is related to the pion-nucleus optical potential via Eq. (3.97). The self-energy $\Pi(q)$ summarizes the entirety of polarization processes induced by the pion in the nucleus. As has been demonstrated in Eqs. (2.9)–(2.12), a knowledge of $\Pi(q)$ leads directly to expressions for a nuclear refractive index and mean-free path for pions moving through a nuclear medium.

We have calculated $\Pi(q)$ by first constructing an equation for its functional derivative with respect to a nucleon propagator $G(k)$ in the medium. This gave us the effective pion-nucleon scattering amplitude $f(kq;kq)$ of Eq. (3.16) that satisfies the modified Chew-Low equation (3.17). In the case of a Fermi sea of noninteracting nucleons, the functional derivative of $\Pi(q)$ with respect to $G(k)$ is proportional to its derivative with respect to the nuclear density. Hence one can easily obtain $\Pi(q)$ in this case by integrating $f(kq;kq)$ over density. Our derivation of the integral equation for $f(kq;kq)$ allows one to extend this amplitude off the pion energy shell. This is a crucial feature, since pion propagation in the nucleus is off shell (see also Ref. 19).

The effective amplitude $f(kq;kq)$ differs from the free-space πN scattering amplitude in several interesting respects:

(i) The pion-nucleon coupling constant is *reduced* in the medium due to the action of the Pauli principle.[58]

(ii) The pion-nucleon threshold is pushed *up* in energy. This is again due to the Pauli principle, which requires that intermediate nucleon states lie outside the Fermi sphere.

(iii) The (3,3) pion-nucleon resonance in $f(kq;kq)$ is narrowed and pushed *up* in energy relative to the free πN resonance as a result of (i) and (ii). This modification of the energy and width of the pion-nucleon (3,3) resonance due to the nuclear medium has not been considered in previous work.[9-19] Our results indicate that these corrections may be important. Equivalently stated, contributions to the pion optical potential of second (and higher) order in the nuclear density appear to be significant.[59]

The pion-nucleus absorption cross section calculated from $f(kq;kq)$ also displays a resonant behavior. The position of this resonance is determined by three competing effects: (i) an upward

shift due to the quenching (renormalization) of the πN coupling constant; (ii) a downward shift due to dispersion in the nuclear medium; and (iii) a downward shift due to the energy dependence of the effective nuclear radius $R+\lambda\!\!\!^{-}$ seen by the pion. The latter effect simulates qualitatively wave-mechanical effects in our otherwise classical estimate of the absorption cross section. Since effects (i) and (ii) tend to cancel (iii), the actual resonance position in pion-nucleus scattering is the result of a rather delicate interplay of several opposing effects.

Except for ^{12}C, there is little information on the *precise* position of the (3, 3) resonance peak in pion-nucleus scattering. The pion mean free path at resonance is found to be small in comparison with the nuclear radius. Consequently, pion absorption is mainly a surface reaction at resonance, and thus subject to nuclear-structure effects that are associated with the nuclear surface. We have attempted to make rough predictions of the expected position of the resonance peak as a function of target mass number A, using an effective surface density $\simeq\frac{2}{3}\rho_{\text{bulk}}$. This is clearly the weakest point in our calculation. A proper calculation of the resonance scattering should employ scattering phase shifts calculated from the Klein-Gordon equation given by Eq. (3.96). Note that the "local density" approximation $n_0 \to \rho(r)$ employed in obtaining the pion-nucleus optical potential of Eq. (3.97) from a nuclear-matter calculation of $\Pi(q)$ is probably quite reliable at the energies of interest in the pion-nucleus scattering problem.

ACKNOWLEDGMENTS

Both of the authors would like to acknowledge the hospitality of Professor M. Jean, M. Veneroni, and the members of the theoretical group of the Institut de Physique Nucleaire at Orsay, where the initial stages of this work were carried out. One of us (CBD) would like to thank the the National Physical Research Laboratory (C.S.I.R.) and the Rand Afrikaans University for travel support and the hospitality enjoyed at these institutions during a visit in August 1971. One of us (CBD) would like to acknowledge useful discussions with members of the theory group at Brookhaven. All numerical calculations were performed on the CDC 6600 at Brookhaven National Laboratory.

---

*Work supported in part by the U. S. Atomic Energy Commission.

[1]F. Binon *et al.*, Nucl. Phys. B17, 168 (1970; J. P. Stroot, in Proceedings of the IVth International Conference on High Energy Physics and Nuclear Structure, Dubna, 1971, edited by V. P. Dzhelepov (Dubna publication No. D16349, 1972), p. 221.

[2]D. T. Chivers *et al.*, Nucl. Phys. A126, 129 (1969); M. M. Kulyakin *et al.*, Dubna Report No. JINR-P1-6131 (to be published).

[3]J. Rohlin *et al.*, Nucl. Phys. B37, 461 (1972); R. W. Bercaw *et al.*, Phys. Rev. Lett. 29, 1031 (1972); C. R. Fletcher *et al.*, Bull. Am. Phys. Soc. 17, 916 (1972).

[4]D. S. Koltun, in *Advances in Nuclear Physics*, edited by M. Baranger and E. Vogt (Plenum, New York, 1969), Vol. 3, p. 11. This review article cites many experimental and theoretical references.

[5]A. A. Carter *et al.*, Nucl. Phys. B26, 445 (1971).

[6]G. Giacomelli, P. Pini, and S. Stagni, CERN-HERA Report No. 69-1, 1969 (unpublished).

[7]A. Rittenberg *et al.*, Rev. Mod. Phys. 43, S114 (1971).

[8]J. S. Ball *et al.*, Phys. Rev. Letters 28, 1143 (1972).

[9]R. M. Sternheimer, Phys. Rev. 101, 384 (1956).

[10]M. M. Sternheim, Phys. Rev. 135, 1364 (1964); M. M. Sternheim and E. H. Auerbach, Phys. Rev. Lett. 25, 1500 (1970); Phys. Rev. C 4, 1805 (1971); R. Silbar and M. M. Sternheim, Phys. Rev. C 6, 764 (1972); L. S. Kisslinger, R. L. Burman, J. H. Koch, and M. M. Sternheim, Phys. Rev. C 6, 469 (1972).

[11]C. Schmit, Lettere Nuovo Cimento 1, 454 (1970); Ph.D. thesis, Orsay, 1971; C. Schmit and J. P. Dedonder, Lettere Nuovo Cimento 1, 191 (1970); J. P. Dedonder, Nucl. Phys. A174, 251 (1971); A180, 472 (1972); J. P. Maillet, C. Schmit, and J. P. Dedonder, Lettere Nuovo Cimento 1, 191 (1970).

[12]C. Wilkin, Lettere Nuovo Cimento 1, 499 (1970); C. Wilkin, CERN Report No. 71-14, 1971 (unpublished), p. 289.

[13]K. Bjornenak *et al.*, Nucl. Phys. B22, 179 (1970); M. Krell and S. Barmo, Nucl. Phys. B20, 461 (1970).

[14]W. B. Jones and J. M. Eisenberg, Nucl. Phys. A154, 49 (1970); L. A. Charlton and J. M. Eisenberg, Ann. Phys. (N.Y.) 63, 286 (1971).

[15]R. Seki, Phys. Rev. C 3, 454 (1971); Bull. Am. Phys. Soc. 17, 917 (1972).

[16]H. K. Lee and H. McManus, Nucl. Phys. A167, 257 (1971); G. W. Edwards and E. Rost, Phys. Rev. Lett. 26, 785 (1971).

[17]M. G. Piepho and G. E. Walker, Bull. Am. Phys. Soc. 17, 589, 917 (1972).

[18]W. R. Gibbs , Phys. Rev. C 3, 1127 (1971); Phys. Rev. C 5, 755 (1972).

[19]R. H. Landau and F. Tabakin, Phys. Rev. D 5, 2746 (1972); R. H. Landau, S. C. Phatak, and F. Tabakin, to be published.

[20]T. E. O Ericson and J. Hüfner, Phys. Lett. 33B, 601 (1970).

[21]T. Kohmura, Nucl. Phys. B36, 228 (1972).

[22]M. P. Locher, O. Steinmann, and N. Straumann, Nucl. Phys. B27, 598 (1971).

[23]A. A. Abrikosov, L. P. Gorkov, and I. E. Dzyaloshinski, *Methods of Quantum Field Theory in Statistical Physics* (Prentice-Hall, Englewood Cliffs, N. J., 1963).

[24]P. Nozières, *The Theory of Interacting Fermi Systems* (Benjamin, New York, 1964).

[25]C. B. Dover, Ann. Phys. 50, 449 (1968).

[26]C. B. Dover, J. Hüfner, and R. H. Lemmer, Ann. Phys. (N.Y.) 66, 248 (1971); C. B. Dover, J. L. Ballot, and R. H. Lemmer, Lettere Nuovo Cimento 2, 715 (1971).

[27]G. F. Chew and F. E. Low, Phys. Rev. 101, 1570 (1956); G. C. Wick, Rev. Mod. Phys. 27, 339 (1955).

[28]J. D. Jackson, *Classical Electrodynamics* (Wiley, New York, 1962). Equation (1.4) is reminiscent of the classical phenomenon of "anomalous dispersion" near a resonance. There is also a qualitative similarity between pion-nucleus scattering in the (3,3) resonance region (short mean free path) and the reflection and absorption of light by a conducting metallic sphere ("the skin effect").

[29]This is actually a matrix product in the nucleon spin-isospin space, $f^\dagger$ being the Hermitian adjoint of f in this space.

[30]S. Schweber, *Relativistic Quantum Field Theory* (Harper and Row, New York, 1964).

[31]Strictly speaking, the orginal derivation (Ref. 27) works with wave functions and commutators and thus yields on-shell amplitudes only.

[32]Alternatively, one could average $f(kq,kq)$ over all nucleon momenta in the Fermi sea and then use Eq. (3.23). This Fermi broadening correction has frequently been discussed (Refs. 4, 10, and 19). In Ref. 19 for instance, it is shown that this correction gives a small energy shift as well as an increase in width. We ignore this energy shift in the present discussion.

[33]Of course, if we include self-energy effects in G, the nucleon will in general be off shell.

[34]S. Barshay, V. Rostokin, and G. Vagradov, to be published.

[35]Note that we have chosen an initial nucleon momentum $\vec{k}=0$. For $k\neq 0$, we get $\tilde{\mu}=[\mu^2+(p_F-k)^2/4]^{1/2}$, so that $\tilde{\mu}$ varies between μ and $(\mu^2+p_F^2/4)^{1/2}$ for $0\leq k\leq p_F$. Thus if we average our amplitude over $\vec{k}$, the average threshold shift will be less than that given by Eq. (3.41).

[36]A preliminary version of this work appeared in C. B. Dover and R. H. Lemmer, Lettere Nuovo Cimento 4, 487 (1972). See also Bull. Am. Phys. Soc. 17, 57 (1972); 17, 917 (1972).

[37]M. Ericson and T. E. O. Ericson, Ann. Phys. (N.Y.) 36, 323 (1966); M. Krell and T. E. O. Ericson, Nucl. Phys. B11, 521 (1969); T. E. O. Ericson, CERN Report No. TH 1093, 1969 (unpublished).

[38]J. M. McKinley, Rev. Mod. Phys. 35, 788 (1963).

[39]Equation (3.57) is the same as Eq. (4.21) of Ref. 26.

[40]One attempts to justify the neglect of crossing terms on the grounds that $A_{33}=\frac{1}{9}\ll 1$. However, the crossing term contributes equally in the coherent amplitude $f_{\rm coh}$ when all channels are considered, so the argument is not convincing. The neglect of crossing also shows up in an unreasonably large value of the momentum cutoff in the integral term in Eq. (3.59); see Sec. IV.

[41]L. Castillejo, R. H. Dalitz, and F. J. Dyson, Phys. Rev. 101, 453 (1956).

[42]Note that, in principle, $\alpha(\omega)$ also depends on $n(\omega)$; see discussion following Eq. (3.30). We neglect this dependence here.

[43]A similar interpretational problem appears in constructing the Chew-Low plot from πN scattering data; see Ref. 27.

[44]The pion lab energy ω_p and the c.m. energy ω_κ are related by $\omega_\kappa+(\kappa^2+m^2)^{1/2}=[\mu^2-m^2+2m(\omega_p+m)]^{1/2}$, where m is the nucleon mass.

[45]G. E. Brown, A. M. Green, W. J. Gerace, and E. M. Nyman, Nucl. Phys. A118, 1 (1968); G. E. Brown, A. M. Green, and W. J. Gerace, Nucl. Phys. A115, 435 (1968); H. Miyazawa, J. Phys. Soc. Japan 19, 1764 (1964).

[46]Equation (3.90) coincides in form and content with Eq. (11.436b) of Ref. 47.

[47]M. L. Goldberger and K. M. Watson, *Collision Theory* (Wiley, New York, 1964).

[48]The pseudopotential concept is restricted to situations where $v\ll\mu^2$ and v changes slowly over a deBroglie wavelength of the pion; see Ref. 47.

[49]H. Feshbach, Ann. Rev. Nucl. Sci. 8, 49 (1958).

[50]A similar procedure has been used for electron waves undergoing multiple scattering in random alloys; see P. W. Anderson and W. L. McMillan, in *Theory of Magnetism in Transition Metals, Proceedings of the International School of Physics "Enrico Fermi," Course 37,* edited by W. Marshall (Academic, New York, 1966), p. 50. The discussion given in this reference and in Eqs. (3.101) to (3.103) supports the use of a complex q in $\Pi(q,\omega)$. The use of only the real part of q in $\Pi(q,\omega)$, as in Ref. 34, does not seem to be consistent. In this case (Ref. 34), the dispersion relation would be written in the form $\omega^2=q^2+\mu^2-k^2\alpha$ rather than (3.100), and one would obtain $\lambda=n_0^2 v_g\tau$ instead of $\lambda=v_g\tau$ as in Eq. (3.103).

[51]These values of p_0 are abnormally high due to the neglect of the crossing term. One expects and gets $p_0\sim m$, when crossing is included (Refs. 27 and 30).

[52]Note that for the finite-density problem, δ does *not* represent the phase shift for pion-nucleus scattering. It is in fact not a measurable quantity, but simply an intermediate construct which enables us to evaluate the pion self-energy. The pion-nucleus phase shifts have then to be extracted from the self-energy in some fashion (quantum mechanically or semiclassically).

[53]Note that this "cross section" is not measurable.

[54]J. M. Blatt and V. F. Weisskopf, *Theoretical Nuclear Physics* (Wiley, New York, 1952), Chap. 8.

[55]*Landolt-Börnstein: Numerical Data and Functional Relationships in Science and Technology,* edited by K.-H. Hellwege (Springer-Verlag, Berlin, 1967), New Series, Group I, Vol. 2, p. 21.

[56]Experimentally, one sees only a small downward shift in $\pi^-+{}^4$He scattering, to a resonance energy of 165 ± 5 MeV (private communication from J. P. Stroot). In the present approach, an effective surface density of $n_0\approx\frac{1}{2}\rho_{\rm bulk}$ would reproduce this shift (see Fig. 26). However, our model (infinite nuclear matter) has very little significance for such a light nucleus.

[57]E. J. Moniz *et al.*, Phys. Rev. Lett. 26, 445 (1971).

[58]Pauli-principle effects in pion-nucleus scattering have also been discussed by H. A. Bethe, Los Alamos Report No. LA5052-MS, 1972 (unpublished).

[59]A very careful calculation of $\pi^-+{}^{12}$C scattering, using a pion optical potential *linear* in the nuclear density, is described in Ref. 19. These authors obtain a peak total cross section at a lab kinetic energy of 115–120 MeV, or about 25–30 MeV *below* the experimental (Ref. 1) peak (see Fig. 10 of Ref. 19). The *upward* shift due to the quenching of the πN coupling constant in the medium would tend to remove this discrepancy.